Published for SISSA by Springer

Received: March 8, 2024
Accepted: June 28, 2024
Published: July 25, 2024

Two-loop anomalous dimensions for small-R jet versus hadronic fragmentation functions

Melissa van Beekveld,[a] **Mrinal Dasgupta**,[b] **Basem Kamal El-Menoufi**,[b,c] **Jack Helliwell**,[d] **Alexander Karlberg**[e] **and Pier Francesco Monni**[e]

[a] *Nikhef, Theory Group, Science Park 105, 1098 XG, Amsterdam, The Netherlands*
[b] *Department of Physics & Astronomy, University of Manchester, Manchester M13 9PL, U.K.*
[c] *School of Physics and Astronomy, Monash University, Wellington Road, Clayton, VIC-3800, Australia*
[d] *Rudolf Peierls Centre for Theoretical Physics, Clarendon Laboratory, Parks Road, University of Oxford, Oxford OX1 3PU, U.K.*
[e] *CERN, Theoretical Physics Department, CH-1211 Geneva 23, Switzerland*

E-mail: mbeekvel@nikhef.nl, mrinal.dasgupta@manchester.ac.uk, basem.el-menoufi@monash.edu, jack.helliwell@physics.ox.ac.uk, alexander.karlberg@cern.ch, pier.monni@cern.ch

Abstract: We study the collinear fragmentation of highly energetic jets defined with a small jet radius. In particular, we investigate how the corresponding fragmentation functions differ from their hadronic counterpart defined in the common $\overline{\text{MS}}$ scheme. We find that the anomalous dimensions governing the perturbative evolution of the two fragmentation functions differ starting at the two loop order. We compute for the first time the new anomalous dimensions at two loops and confirm our predictions by comparing the inclusive small-R jet spectrum against a fixed order perturbative calculation at $\mathcal{O}(\alpha_s^2)$. To investigate the dependence of the anomalous dimension on the kinematic cutoff variable, we study the fragmentation functions of Cambridge jets defined with a transverse momentum cutoff as opposed to an angular cutoff R. We further study the evolution of the small-R fragmentation function with an alternative cutoff scale, proportional to zR, representing the maximum possible transverse momentum of emissions within a jet. In these cases we find that the two-loop anomalous dimensions coincide with the $\overline{\text{MS}}$ DGLAP ones, highlighting a correspondence between the $\overline{\text{MS}}$ scheme and a transverse-momentum cutoff.

Keywords: Jets and Jet Substructure, Resummation

ArXiv ePrint: 2402.05170

https://doi.org/10.1007/JHEP07(2024)239

JHEP07(2024)239

Contents

1 Introduction

The increasing precision reached by the LHC experiments in the measurement of the properties of QCD jets necessitates higher accuracy in perturbative calculations of jet observables. In addition to higher-order fixed-order calculations, multi-scale observables commonly also require the resummation of logarithmically enhanced radiative corrections of infrared origin. In the latter context, we consider the problem of timelike collinear fragmentation of hard partons produced in a high-energy scattering process. In this regime we are concerned with observables sensitive solely to collinear logarithmic corrections, where the leading logarithms (LL) are single logarithms $\alpha_s^n L^n$. Observables of this class are common in collider physics and have been extensively studied in the literature (see e.g. [1–23]).

For such single-logarithmic observables, a next-to-leading-logarithmic (NLL) calculation would capture the next-to-single logarithmic tower of corrections of order $\alpha_s^n L^{n-1}$. Here the general formulation of an algorithm to carry out NLL resummations requires the consistent inclusion of $1 \to 3$ splitting functions at tree-level along with the one-loop corrections to the $1 \to 2$ splitting functions. A possible theoretical approach to such resummation algorithms can be formulated using the language of generating functionals [24–26], tailored to this class of fragmentation problems in refs. [10, 22]. Such a formulation is rather powerful when trying to connect the field of QCD resummation with that of parton showers, with which the generating functional method is intimately linked.

An important aspect of the development of novel resummation techniques is testing them across observables sensitive to different aspects of fragmentation. For example, ref. [22] considered the NLL calculation of a family of groomed angularities and fractional moments of

JHEP07(2024)239

energy correlators. These observables are of a more inclusive kind in that they are defined by integrating over the momentum fraction z of a given collinear splitting. As a next natural step, we wish to consider observables that are *differential* in z, to probe more deeply the structure of our formulation. Observables belonging to this class are the common NLO fragmentation functions (FFs) measured either on final state hadrons [4, 5] or on final state jets clustered with a small jet radius $R \ll 1$, which have been studied for instance in refs. [10, 12, 13]. These observables are sensitive to both the z dependence of the novel anomalous dimension $\mathcal{B}_2^f(z)$ computed for quark and gluon jets respectively in refs. [16, 22], as well as to the full triple-collinear $1 \to 3$ squared splitting amplitudes [27, 28].

In the process of testing our formulation on such observables we have uncovered an important conceptual subtlety connected to FFs defined with an angular cutoff R. In particular, we find that the anomalous dimensions of small-R FFs differ from the standard DGLAP ones starting at the two loop order $\mathcal{O}(\alpha_s^2)$. To the best of our knowledge there has been no previous calculation of the two loop anomalous dimensions for small-R jets, in previous literature the answer at this order was conjectured from the form of the evolution equation (see e.g. ref. [13]).

Interestingly, the two-loop difference between these anomalous dimensions takes a rather simple analytic form with a universal structure across flavour channels. Moreover, the term that breaks the correspondence between small-R jets and timelike DGLAP evolution is of the same form and related analytic origin as the term identified first by Curci, Furmanski, and Petronzio [5] responsible for breaking of the Gribov-Lipatov reciprocity relation [29–32] between timelike and spacelike anomalous dimension in the non-singlet flavour channel. In ref. [33] it was argued that terms of this type are linked to the choice of the evolution cutoff (see also related discussions in ref. [34]). It is therefore also interesting to explore the link with FFs defined by other types of kinematical cuts, e.g. a transverse momentum. In order to investigate this observation, we compute the two-loop evolution kernels for Cambridge jets defined with a transverse momentum y_{cut} cutoff. We further compute a variant of the small-R FF, where the kinematic cut on the radiation is proportional to $z\,R$ (with z being the energy fraction of the jet), related to the maximum possible transverse momentum of emissions within a small-R jet. Remarkably, in both of these cases we find that the two-loop anomalous dimensions now coincide with DGLAP. This result is critical to understand how to reproduce DGLAP evolution beyond LO in parton showers, which inevitably use a kinematical cutoff.[1]

In this article we present the new anomalous dimensions for small-R FFs at the two-loop order and confirm our predictions by comparing to an exact numerical fixed order calculation at $\mathcal{O}(\alpha_s^2)$. The paper is organised as follows. In section 2 we study the $\overline{\text{MS}}$ fragmentation function and we analyse the effect of placing an angular cutoff $R \ll 1$. We then present a simple recipe to derive the small-R anomalous dimensions at the two-loop order. In section 3 we consider the inclusive small-R jet spectrum as a case study and test our findings against a fixed-order calculation at $\mathcal{O}(\alpha_s^2)$ using the EVENT2 program [36]. To investigate the dependence of the anomalous dimensions on the kinematic cutoff, we also report the study of the FF at $\mathcal{O}(\alpha_s^2)$ with a transverse momentum cutoff in section 3.1, as well as the study of the small-R jet FF with a modified transverse-momentum-like cutoff scale. In these

[1] See also ref. [35] and related work for investigations in a related direction.

JHEP07(2024)239

cases the anomalous dimensions coincide with the DGLAP ones, highlighting an important correspondence between the $\overline{\text{MS}}$ scheme and a transverse-momentum cutoff at the NLL order. Finally, our conclusions are presented in section 4. We also include three appendices which present: some relevant technical details in appendix A, our full set of modifications to the DGLAP anomalous dimensions in appendix B, and a derivation of the anomalous dimensions from the formalism of ref. [22] in appendix C.

2 The inclusive microjet spectrum and small-R fragmentation function

We consider the inclusive small-R jets (microjets) fragmentation function which, for illustrative purposes, we define in the process $e^+e^- \to$ jets. The cross section differential in the energy fraction z carried by a microjet is given, up to power corrections, by

$$\frac{1}{\sigma_0}\frac{d\sigma^{\text{jet}}}{dz} \equiv \sum_{i=q,\bar{q},g} \int_z^1 \frac{d\xi}{\xi} C_i^{\text{jet}}\left(\xi,\mu,Q\right) D_i^{\text{jet}}\left(\frac{z}{\xi},\mu,E\,R\right) , \tag{2.1}$$

with σ_0 denoting the Born cross section for $e^+e^- \to q\bar{q}$. The matching coefficient $C_i^{\text{jet}}\left(\xi,\mu,Q\right)$ admits a fixed order perturbative expansion in $\alpha_s(\mu)$. We take μ to be of the order of the centre-of-mass energy Q and more precisely we will set $\mu = E = Q/2$, i.e. the energy of each hemisphere. For this scale, the fragmentation function $D_i^{\text{jet}}\left(\frac{z}{\xi},\mu,E\,R\right)$ resums the logarithms of the small jet radius. Its evolution with the factorisation scale μ is perturbative as long as $Q\,R \gg \Lambda_{\text{QCD}}$ and it is governed by the equation

$$\frac{dD_k^{\text{jet}}\left(z,\mu,E\,R\right)}{d\ln\mu^2} = \sum_i \int_z^1 \frac{d\xi}{\xi} \hat{P}_{ik}\left(\frac{z}{\xi},\mu,E\,R\right) D_i^{\text{jet}}\left(\xi,\mu,E\,R\right) . \tag{2.2}$$

Here the index i runs over all active quarks, antiquarks, and gluons. The main result of this article is that, up to NLL the anomalous dimension $\hat{P}$ admits a perturbative expansion of the form

$$\begin{aligned}
\hat{P}_{ik}\left(z,\mu,E\,R\right) &= \frac{\alpha_s(\mu^2)}{2\pi}\left(\hat{P}_{ik}^{(0)}(z) + \frac{\alpha_s(\mu^2)}{2\pi}\hat{P}_{ik}^{(1),\,\text{AP}}(z) - \frac{\alpha_s(E^2R^2)}{2\pi}\delta\hat{P}_{ik}^{(1)} + \mathcal{O}(\text{NNLL})\right) \\
&= \frac{\alpha_s(\mu^2)}{2\pi}\left(\hat{P}_{ik}^{(0)}\left(z\right) + \frac{\alpha_s(\mu^2)}{2\pi}\hat{P}_{ik}^{(1)}\left(z\right)\right. \\
&\qquad \left. - \left(\frac{\alpha_s(E^2R^2)}{2\pi} - \frac{\alpha_s(\mu^2)}{2\pi}\right)\delta\hat{P}_{ik}^{(1)}\left(z\right) + \mathcal{O}(\text{NNLL})\right) .
\end{aligned} \tag{2.3}$$

As we will show below, while at one loop the anomalous dimension $\hat{P}_{ik}^{(0)}$ agrees with the Altarelli-Parisi one, which we denote with $\hat{P}_{ik}^{(n),\,\text{AP}}(z)$ here, this is not true any longer at higher orders. In particular, we will show that $\hat{P}_{ik}^{(1)}(z) = \hat{P}_{ik}^{(1),\,\text{AP}}(z) - \delta\hat{P}_{ik}^{(1)}(z)$, where the new term $\delta\hat{P}_{ik}^{(1)}(z)$ is a consequence of clustering effects, which are absent in conventional $\overline{\text{MS}}$ evolution of the FFs. Eq. (2.2) is solved as a path-ordered exponential describing the evolution between a hard scale $\mu = E$ and a low scale $\mu = E\,R$, at which the solution is convoluted with a boundary condition $D_k^{\text{jet}}\left(z,E\,R,E\,R\right)$. A LL resummation of the FF would

JHEP07(2024)239

require the one-loop kernels, while the two-loop kernels as well as the one-loop correction to the boundary condition are required at NLL.

To define the small-R jets we work with the *inclusive* generalised-k_t family of algorithms [37], which cluster sequentially proto-jets according to the distance measure

$$d_{ij} = 2 \min\left(\frac{E_i^2}{Q^2}, \frac{E_j^2}{Q^2}\right)^p (1 - \cos\theta_{ij}),$$
$$d_{iB} = \frac{E_i^{2\,p}}{Q^{2\,p}} R^2, \tag{2.4}$$

where E_i denotes the energy of proto-jet i and θ_{ij} is the angle between proto-jets i and j. The algorithm proceeds by finding the smallest between all d_{ij} and d_{iB} in the event and recombining either i and j if d_{ij} is the smallest distance or promoting i to a jet if d_{iB} is the smallest distance. The proto-jets are recombined according to the E scheme, in which the four momenta are added together. The parameter p identifies the algorithm, with $p = 1$ corresponding to the k_t algorithm [38], $p = -1$ to anti-k_t [39] and $p = 0$ to the Cambridge/Aachen (C/A) algorithm [40, 41]. Though we explicitly study the Cambridge-Aachen algorithm, at NLL the considerations that follow will hold for all of the three algorithms. This is because in the small-R limit, differences between these three algorithms only arise in kinematic configurations that contribute starting at NNLL. In the case of SISCone [42], the only difference at the NLL order is entirely encoded in the boundary condition to the evolution equation (2.2), while the anomalous dimensions are identical to those of the inclusive generalised-k_t family of jet algorithms.

The all-order structure of eq. (2.2) is closely related to that of the standard fragmentation function, governed by the DGLAP equation [1–3]. However, because of a subtlety we will discuss in the following, the anomalous dimensions governing the evolution of D_i^{jet} will differ from the DGLAP anomalous dimension describing the evolution of the $\overline{\text{MS}}$ fragmentation function starting at the two-loop order. This implies that while $\hat{P}_{ik}^{(0)}(z) = \hat{P}_{ik}^{(0),\,\text{AP}}(z)$ in eq. (2.3), this is not true at higher orders in α_s. In the following section we will derive the one-loop matching coefficients needed at NLL, while in section 2.2 we will compute the new two-loop anomalous dimension. Finally, in section 2.3 we will discuss the running coupling of the new term $\delta\hat{P}_{ik}^{(1)}(z)$ along with the physical interpretation of this effect. Appendix C reports a derivation of the final evolution equation (2.2) using the formalism of ref. [22].

2.1 One loop matching coefficients and boundary conditions

We start with a simple $\mathcal{O}(\alpha_s)$ calculation of eq. (2.1), which will allow us to extract the one-loop matching coefficients C_i^{jet} as well as the boundary condition to eq. (2.2), both of which are needed for a NLL calculation.

At $\mathcal{O}(\alpha_s)$, we start with the production of a $q\bar{q}g$ final state, and consider the action of a clustering algorithm into small-R jets. Since we work in the limit $R \ll 1$ we only need to consider kinematic configurations enhanced by a collinear singularity (hence producing logarithms of R). This simply amounts to configurations in which the gluon is collinear to either of the two quarks. The resulting calculation is thus identical to that of the standard fragmentation function in the regions $\theta_{qg}^2 > R^2$ and $\theta_{\bar{q}g}^2 > R^2$, but it gets modified when

JHEP07(2024)239

the gluon is recombined with one of the quarks. At the one-loop order, this modification effectively replaces the $\mathcal{O}(\epsilon^{-1})$ pole of the $\overline{\text{MS}}$ fragmentation function with $\ln 1/R$ and it will produce a low-scale non-logarithmic term, which serves as a boundary condition at $\mu = E\,R$. For the generalised-k_t family of algorithms, we obtain

$$D_i^{\text{jet}}(z,\mu,E\,R) = \delta(1-z) + \frac{\alpha_s(\mu)}{2\pi}\, D_i^{\text{jet}\,(0)}(z,\mu,E\,R) + \mathcal{O}(\alpha_s^2)\,, \tag{2.5}$$

where

$$\begin{aligned} D_q^{\text{jet}\,(0)}(z,E\,R,E\,R) &= -2\,C_F\,(1+z^2)\left(\frac{\ln(1-z)}{1-z}\right)_+ \\ &\quad + C_F\left(-1+2\left(2-\frac{2}{z}-z\right)\ln(1-z) + \left(6-\frac{4}{(1-z)\,z}\right)\ln z\right) \\ &\quad + C_F\left(\frac{13}{2}-\frac{2}{3}\,\pi^2\right)\delta(1-z)\,, \end{aligned} \tag{2.6}$$

$$D_{\bar q}^{\text{jet}\,(0)}(z,E\,R,E\,R) = D_q^{\text{jet}\,(0)}(z,E\,R,E\,R)\,, \tag{2.7}$$

$$\begin{aligned} D_g^{\text{jet}\,(0)}(z,E\,R,E\,R) &= 2\left(\hat P_{gg}^{(0)}(z) + 2\,n_f\,\hat P_{qg}^{(0)}(z)\right)\ln\frac{1}{z} - 4\,C_A\,\frac{\left(1-z+z^2\right)^2}{z}\left(\frac{\ln(1-z)}{1-z}\right)_+ \\ &\quad - 4\,n_f\,\hat P_{qg}^{(0)}(z)\,\ln(1-z) - 4\,T_R\,n_f\,z\,(1-z) \\ &\quad + \left(C_A\left(\frac{67}{9}-\frac{2}{3}\,\pi^2\right) - T_R\,n_f\,\frac{23}{9}\right)\delta(1-z)\,. \end{aligned} \tag{2.8}$$

Here we defined the regularised splitting kernels $\hat P_{gg}^{(0)}(z)$ and $\hat P_{qg}^{(0)}(z)$ as

$$\hat P_{qg}^{(0)} = T_R\left(z^2+(1-z)^2\right)\,, \quad \hat P_{gg}^{(0)} = 2\,C_A\left(\frac{z}{(1-z)_+} + \frac{1-z}{z} + z\,(1-z)\right) + b_0\,\delta(1-z)\,, \tag{2.9}$$

with $b_0 = 11/6\,C_A - 2/3\,T_R\,n_f$, $C_F = 4/3$, $T_R = 1/2$ and $C_A = 3$, while n_f is the number of light-quark flavours, assumed to be 5 here.

The above expressions agree with the results of ref. [13].[2] Finally, the matching coefficients C_i^{jet} are simply obtained by matching the calculation of D_i^{jet} to the full QCD calculation at one loop [5], the result is also given in eq. (2.16) of [45]. At this order, they agree with the sum of longitudinal and transverse coefficient functions entering the $\overline{\text{MS}}$ fragmentation function which were first computed in ref. [5]. These read

$$C_i^{\text{jet}}(z,\mu,Q) = \delta(1-z) + \frac{\alpha_s(\mu)}{2\pi}\, C_i^{\text{jet}\,(0)}(z,\mu,Q) + \mathcal{O}(\alpha_s^2)\,, \tag{2.10}$$

[2]We find a different result for the SISCone algorithm already at $\mathcal{O}(\alpha_s)$, which can be traced back to an initial error in refs. [13, 43], later corrected in ref. [44]. Our results agree with the latter, and therefore we refrain from reporting them here.

JHEP07(2024)239

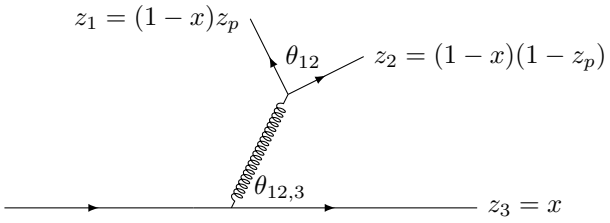

Figure 1. Phase space parametrisation for the production of two identical quarks, labelled by particles 1 and 3.

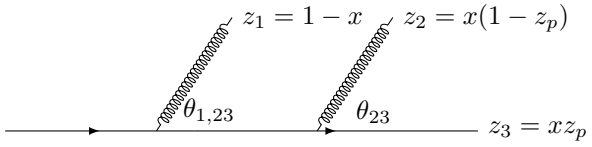

Figure 2. Phase space parametrisation for the radiation of two independent gluons off a quark line.

where, setting $\mu = E$,

$$C_q^{\text{jet}\,(0)}(z,E,Q) = C_F\,(1+z^2)\left(\frac{\ln(1-z)}{1-z}\right)_+ - C_F\left(\frac{3}{2} - 2\,(1+z^2)\ln 2\right)\left(\frac{1}{1-z}\right)_+ + \frac{C_F}{2}\left(5 - 3\,z + 4\,\frac{(1+z^2)}{1-z}\,\ln z\right) - C_F\left(\frac{9}{2} - \frac{2}{3}\,\pi^2 - 3\ln 2\right)\delta(1-z)\,, \tag{2.11}$$

$$C_{\bar{q}}^{\text{jet}\,(0)}(z,E,Q) = C_q^{\text{jet}\,(0)}(z,E,Q)\,, \tag{2.12}$$

$$C_g^{\text{jet}\,(0)}(z,E,Q) = 2\,C_F\,\frac{2-2\,z+z^2}{z}\,(\ln(1-z) + 2\,\ln z + 2\,\ln 2)\,. \tag{2.13}$$

2.2 The two-loop anomalous dimensions

We can now proceed with the analysis at the two-loop order, by calculating the splitting kernels $\hat{P}_{ik}^{(1)}$. For ease of presentation, we use a simple method for the calculation of the two-loop anomalous dimension in the non-singlet (NS) flavour channel, where we target the C_F^2 colour structure and hence set for the time being $C_A = n_f = 0$. It will then be evident how this argument can be generalised to the remaining colour and flavour channels, allowing us to derive the full anomalous dimension at two loops.

2.2.1 The C_F^2 contribution to the NS channel

Since for the time being we are interested in the C_F^2 contribution to the NS channel, we must take into account the abelian collinear splittings depicted in figure 1 ($q \to qq\bar{q}$ — with identical quark flavours) and figure 2 ($q \to qgg$), whose spin-averaged kernels $\langle P \rangle$ in the triple collinear limit can be found in refs. [27, 28, 46, 47]. To extract the C_F^2 contribution to the two loop splitting kernel $\hat{P}_{qq}^{(1)}$, it is convenient to start from the identical-quark contribution

JHEP07(2024)239

to the standard FF (i.e. not for small-R jets) depicted in figure 1. For $z \neq 1$ this reads

$$I^{\text{id.}}_{C_F^2}(\epsilon, z) \equiv \frac{1}{2!} \int d\Phi_3^{(A)} \frac{(8\pi\,\bar{\alpha}_s \mu^{2\epsilon})^2}{s_{123}^2} \langle P \rangle_{C_F\,(C_F - C_A/2)} \left(\delta(z - (1-x)z_p) + \delta(x - z)\right) , \quad (2.14)$$

where the identical-fermion contribution to the $1 \to 3$ splitting function $\langle P \rangle_{C_F\,(C_F - C_A/2)}$ is given in eq. (31) of ref. [28]. The coupling α_s is renormalised in the $\overline{\text{MS}}$ scheme and we used the short-hand notation $\bar{\alpha}_s \equiv S_\epsilon^{-1}\,\alpha_s$, with $S_\epsilon = (4\pi)^\epsilon\, e^{-\epsilon\gamma_E}$. The phase space measure $d\Phi_3^{(A)}$ is defined in appendix A, s_{123} is the squared invariant mass of the collinear three-parton system, and the two δ functions correspond to fixing the energy fraction of either of the two final state quarks contributing to the NS FF. The two contributions are identical and exactly cancel the $1/2!$ symmetry factor. The integration is straightforward and the result can be found, for instance, in ref. [16] (and specifically by multiplying eq. (3.7) in this reference by a factor $-1/\epsilon$). The single pole directly contributes to the NLO DGLAP anomalous dimension in the non-singlet channel.

The next step is then to consider the same contribution to the small-R FF. An important property of the integral (2.14) is that it contributes only a single pole to the FF, and it does not receive a contribution from virtual corrections. This is reflected in the fact that there is no collinear singularity when the final state particles are strongly ordered in angle. We then consider applying the C/A clustering which, in the limit $R \ll 1$, will only modify eq. (2.14) in configurations where the relative angles become small. Due to the absence of a collinear enhancement in such configurations, the contribution of such regions is power suppressed in R^2. This immediately implies that the contribution from this channel to the small-R two loop anomalous dimension $\hat{P}_{qq}^{(1)}$ will coincide with the corresponding DGLAP counterpart.

Next, we consider the abelian channel, namely the double-real contribution in figure 2, and corresponding real-virtual corrections. As before we start by examining its contribution to the hadronic FF. One can single out the two loop correction to the Altarelli-Parisi splitting kernel by calculating the following combination

$$\begin{aligned} I^{\text{ab.}}_{C_F^2}(z, \epsilon) \equiv\; & \frac{1}{2!} \int d\Phi_3^{(B)} \frac{(8\pi\,\bar{\alpha}_s \mu^{2\epsilon})^2}{s_{123}^2} \langle P \rangle_{C_F^2}\, \delta(z - x z_p) \\ & + \int \frac{d\theta^2}{\theta^2}\, dx\, \frac{\alpha_s^2}{(2\pi)^2}\, \mathcal{V}^{(1),C_F^2}_{q\to qg}(x, \theta, \epsilon)\, \delta(x - z) \\ & - \frac{1}{2!} \int d\Phi_2^2 \frac{(8\pi\,\bar{\alpha}_s \mu^{2\epsilon})^2}{E^4} \frac{P_{qq}^{(0)}(x, \epsilon)}{\theta_{13}^2} \frac{P_{qq}^{(0)}(z_p, \epsilon)}{\theta_{23}^2} \delta(z - x z_p) , \qquad z \neq 1 , \end{aligned} \quad (2.15)$$

where the phase space measure $d\Phi_3^{(B)}$ is given in appendix A, and the abelian contribution to the $1 \to 3$ splitting function $\langle P \rangle_{C_F^2}$ can be found in eq. (33) of ref. [28].[3] Finally, the one-loop correction to the $1 \to 2$ splitting function $\mathcal{V}^{(1),C_F^2}_{q\to qg}$ was calculated in ref. [46] and in the convention of eq. (2.15) is given in the r.h.s. of eq. (3.42) of ref. [16] with a factor of $\alpha_s^2/(2\pi)^2$ removed. The term in the third line of eq. (2.15) has the role of subtracting the LL terms from the first two lines, hence cancelling all contributions originating from configurations strongly ordered in angle. The $d\Phi_2^2$ phase space measure is defined starting

[3] We note that the overall C_F^2 colour factor is included in $\langle P \rangle_{C_F^2}$ in our notation.

JHEP07(2024)239

from the iteration of the $1 \to 2$ phase space and it is given by

$$d\Phi_2^2 \equiv \frac{E^{4-4\epsilon}}{(4\pi)^{4-2\epsilon}\Gamma(1-\epsilon)^2}\, d\theta_{13}^2\, d\theta_{23}^2\, dx\, dz_p\, \theta_{13}^{-2\epsilon}\theta_{23}^{-2\epsilon}(x(1-x))^{-2\epsilon}(z_p(1-z_p))^{-2\epsilon}\,. \tag{2.16}$$

We can recast eq. (2.15) as (for $z \neq 1$)

$$\begin{aligned} I^{\text{ab.}}_{C_F^2}(z,\epsilon) = {} & \frac{1}{2!}\int d\Phi_3^{(B)}(8\pi\bar{\alpha}_s\mu^{2\epsilon})^2 \left(\frac{1}{s_{123}^2}\langle P\rangle_{C_F^2} - \frac{\mathcal{J}(x,z_p)}{E^4}\frac{P_{qq}^{(0)}(x,\epsilon)}{\theta_{13}^2}\frac{P_{qq}^{(0)}(z_p,\epsilon)}{\theta_{23}^2}\right)\delta(z-xz_p) \\ & + \int \frac{d\theta^2}{\theta^2}\, dx\, \frac{\alpha_s^2}{(2\pi)^2}\, \mathcal{V}_{q\to qg}^{(1),C_F^2}(x,\theta,\epsilon)\,\delta(x-z) \\ & + \frac{1}{2!}\left(\int d\Phi_3^{(B)}\,\mathcal{J}(x,z_p) - \int d\Phi_2^2\right)\frac{(8\pi\,\bar{\alpha}_s\mu^{2\epsilon})^2}{E^4}\frac{P_{qq}^{(0)}(x,\epsilon)}{\theta_{13}^2}\frac{P_{qq}^{(0)}(z_p,\epsilon)}{\theta_{23}^2}\,\delta(z-xz_p)\,, \end{aligned} \tag{2.17}$$

where the prefactor $\mathcal{J}(x,z_p)$ is given by

$$\mathcal{J}(x,z_p) \equiv \frac{1}{z_1 z_2 z_3 x} = \frac{1}{(1-x)x^3(1-z_p)z_p}\,. \tag{2.18}$$

To make contact with the small-R FF, we partition the three-body phase space according to the Cambridge-Aachen algorithm, that is we trade the $1/2!$ in the double-real radiation integrals by an angular-ordering condition $\Theta(\theta_{13}^2 - \theta_{23}^2)$. In considering the action of the jet algorithm we are allowed to neglect two effects which are subleading for the present analysis. The first is the contribution from configurations where the jet algorithm clusters emissions in regions of phase space that are free of collinear singularities (e.g. when the two gluons in figure 2 are first clustered together). These clustering corrections are power suppressed in R^2 and therefore can be neglected in the small-R limit. The second effect that we can neglect in the calculation performed below is the recoil of the jet axis due to recombination kinematics following a clustering. We have checked by explicit computation that this effect amounts to a contribution to the boundary condition at $\mathcal{O}(\alpha_s^2)$, and therefore is subleading w.r.t. the accuracy considered here.

We now discuss the effect of the clustering on each of the terms in eq. (2.17). Due to the subtraction of the strongly-ordered regime, the first term in eq. (2.17) enjoys the same properties as the identical-quark correction in eq. (2.14), in that it is free of soft and collinear divergences. For this reason, any region of phase space where jet clustering is active gives only a power suppressed contribution $\mathcal{O}(R^2)$. This again implies that the corresponding contribution to the splitting kernel $\hat{P}_{qq}^{(1)}$ is the same for the DGLAP and small-R cases.

We next consider the second and third line of eq. (2.17). It is convenient to split the real phase space integrals by introducing the partition of unity

$$1 = \Theta(\theta_{13}^2 - R^2) + \Theta(R^2 - \theta_{13}^2)\,. \tag{2.19}$$

Analogously, for the virtual corrections $\mathcal{V}_{q\to qg}^{(1),C_F^2}$ we insert $1 = \Theta(\theta^2 - R^2) + \Theta(R^2 - \theta^2)$. Accordingly, we can write

$$I^{\text{ab.}}_{C_F^2}(z,\epsilon) = I^{\text{ab.}}_{>R^2}(z,\epsilon) + I^{\text{ab.}}_{<R^2}(z,\epsilon)\,. \tag{2.20}$$

JHEP07(2024)239

We now consider the calculation of each of the above two terms, starting with the contribution $I^{\text{ab.}}_{<R^2}(z,\epsilon)$. In this case, every emission is contained inside the jet. Hence the sum of the second and third line of eq. (2.17) only contributes a $\delta(1-z)$ to the small-R FF, which does not have any $\ln 1/R^2$ enhancement and hence amounts to a subleading, NNLL boundary condition. Secondly, we focus on the term $I^{\text{ab.}}_{>R^2}(z,\epsilon)$. The only source of difference between the small-R and DGLAP anomalous dimensions is due to the third line in eq. (2.17) in a region where $\theta_{23}^2 < R^2$ while $\theta_{13}^2 > R^2$. In this case, we can directly calculate the difference between the DGLAP and small-R anomalous dimensions by evaluating the integral

$$\left(\int d\Phi_3^{(B)}\,\mathcal{J}(x,z_p) - \int d\Phi_2^2\right)\frac{(8\pi\,\bar{\alpha}_s\mu^{2\epsilon})^2}{E^4}\,\frac{P_{qq}^{(0)}(x,\epsilon)}{\theta_{13}^2}\,\frac{P_{qq}^{(0)}(z_p,\epsilon)}{\theta_{23}^2}\,\Theta(\theta_{13}^2-R^2)\Theta(R^2-\theta_{23}^2)$$
$$\times\,(\delta(z-xz_p)-\delta(z-x)) = \frac{\alpha_s^2}{(2\pi)^2}\left(\delta\hat{P}_{qq}^{(1)}(z)\ln\frac{1}{R^2}+\mathcal{O}(\epsilon)\right), \tag{2.21}$$

where the two δ functions encode the difference between the hadronic and small-R jet FF. In obtaining the above equation we have made use of the fact that the contribution of the virtual corrections $\mathcal{V}_{q\to qg}^{(1),C_F^2}$ is common to both FFs and thus it cancels. Eq. (2.21) reveals that the non-singlet contribution to the two-loop anomalous dimension for the small-R FF can be obtained from the corresponding DGLAP splitting kernel by subtracting the quantity $\delta\hat{P}_{qq}^{(1)}(z)$, namely

$$\hat{P}_{qq}^{(1)}(z) = \hat{P}_{qq}^{(1),\,\text{AP}}(z) - \delta\hat{P}_{qq}^{(1)}(z)\,, \tag{2.22}$$

where we denote by $\hat{P}_{qq}^{(1),\,\text{AP}}(z)$ the standard DGLAP evolution kernels, and[4]

$$\begin{aligned}\delta\hat{P}_{qq}^{(1)}(z) &\equiv \left(2\,\ln z\,\hat{P}_{qq}^{(0)}\right)\otimes\hat{P}_{qq}^{(0)}\\ &= -C_F^2\,\ln z\left(\frac{3\,z^2+1}{1-z}\ln z - 4\frac{1+z^2}{1-z}\ln(1-z) - \frac{z(4+z)+1}{1-z}\right),\end{aligned} \tag{2.23}$$

with

$$\hat{P}_{qq}^{(0)}(z) = C_F\,(1+z^2)\left(\frac{1}{1-z}\right)_+ + C_F\,\frac{3}{2}\,\delta(1-z)\,. \tag{2.24}$$

The remarkably simple structure of the result can be understood by inspecting eq. (2.21). Here, the difference between the two phase space measures $d\Phi_3^{(B)}$ and $d\Phi_2^2$ is of $\mathcal{O}(\epsilon\,\ln x)$, arising from the extra $x^{-2\epsilon}$ factor in the D-dimensional three-body phase space $d\Phi_3^{(B)}$. This multiplies a $1/\epsilon$ pole of collinear origin arising from the $\theta_{23}\to 0$ limit, giving a finite leftover. Finally, the difference between the two δ functions in eq. (2.21) is reflected in the regularised splitting functions in eq. (2.23).

The above result is the central observation of this article. It highlights a difference between the anomalous dimension governing standard DGLAP evolution and that of a fragmentation function defined with an angular cutoff. It is noteworthy that this term looks precisely like the difference between the timelike and the spacelike two-loop splitting kernels [5] that breaks the reciprocity relation [30–33] between timelike and spacelike anomalous dimensions. The origin of this term was previously found to be related to the specific kinematic infrared cutoff

[4]The standard convolution operator is defined as $f(z)\otimes g(z)\equiv\int_z^1 d\,x/x\,f(x)\,g(z/x)$.

JHEP07(2024)239

(e.g. angular vs. transverse momentum) in the collinear radiation [32]. To investigate the correspondence of the anomalous dimensions with the kinematic cutoff, in section 3.1 we will calculate and test the two-loop anomalous dimensions for the fragmentation functions of Cambridge jets, defined with a transverse-momentum cutoff.

2.2.2 Generalisation to all colour and flavour channels

The arguments outlined above can be generalised to other flavour channels. In general, starting at two loops, a given entry to the anomalous dimension matrix for the small-R FF will take the form

$$\hat{P}_{ik}^{(1)} = \hat{P}_{ik}^{(1),\,\mathrm{AP}} - \delta\hat{P}_{ik}^{(1)}\,. \tag{2.25}$$

To calculate $\delta\hat{P}_{ik}^{(1)}$, we observe that it originates from a sequence of two collinear splittings in which an $\mathcal{O}(\epsilon)$ contribution to the first splitting (which amounts to the leading-order splitting function multiplied by a $\ln z$ factor coming from the expansion of the D dimensional phase space measure) is convoluted with the $\mathcal{O}(\epsilon^{-1})$ pole term of the second splitting (amounting to the corresponding leading-order splitting function). Concretely, we consider the sequence of $1 \to 2$ splittings originating from the fragmentation of a parton A, i.e.

$$A \to BC \to (DE)\,C\,, \quad A \to BC \to B\,(FG)\,. \tag{2.26}$$

The above sequences will then contribute to the following anomalous dimensions

$$\begin{aligned}
\delta\hat{P}_{EA}^{(1)}(z) &\equiv \left(2\,\ln z\,\hat{P}_{BA}^{(0)}\right) \otimes \hat{P}_{EB}^{(0)}\,; & \delta\hat{P}_{DA}^{(1)}(z) &\equiv \left(2\,\ln z\,\hat{P}_{BA}^{(0)}\right) \otimes \hat{P}_{DB}^{(0)}\,,\\
\delta\hat{P}_{GA}^{(1)}(z) &\equiv \left(2\,\ln z\,\hat{P}_{CA}^{(0)}\right) \otimes \hat{P}_{GC}^{(0)}\,; & \delta\hat{P}_{FA}^{(1)}(z) &\equiv \left(2\,\ln z\,\hat{P}_{CA}^{(0)}\right) \otimes \hat{P}_{FC}^{(0)}\,,
\end{aligned} \tag{2.27}$$

where the sum over the intermediate states, i.e. over the indices B and C, in each channel is understood. The relevant corrections $\delta\hat{P}_{ik}^{(1)}$ at the two loop order are reported in appendix B. A crucial property of the extra terms in the small-R anomalous dimensions is that they must satisfy the sum rules. Using the expressions given in appendix B we consistently find

$$\begin{aligned}
\int_0^1 d\,z\,z\,\left(\delta\hat{P}_{qq}^{(1)}(z) + \delta\hat{P}_{gq}^{(1)}(z) + \delta\hat{P}_{\bar{q}q}^{(1)}(z)\right) &= 0\,,\\
\int_0^1 d\,z\,z\,\left(\delta\hat{P}_{gg}^{(1)}(z) + \delta\hat{P}_{qg}^{(1)}(z) + \delta\hat{P}_{\bar{q}g}^{(1)}(z)\right) &= 0\,,\\
\int_0^1 d\,z\,\left(\delta\hat{P}_{qq}^{(1)}(z) - \delta\hat{P}_{\bar{q}q}^{(1)}(z)\right) &= 0\,.
\end{aligned} \tag{2.28}$$

2.3 Running coupling effects beyond two loops

In this section we will discuss the scale of the coupling multiplying $\hat{P}_{ik}^{(1)}(z)$ in the evolution equation of the small-R FFs shown in eq. (2.2). Here we will present a simple physical argument to justify the expression given in eq. (2.3). A full derivation of this equation leading to the explicit scale of the coupling for the term proportional to $\delta\hat{P}_{ik}^{(1)}(z)$ is reported in appendix C. As shown explicitly in the previous section, the two loop anomalous dimension $\hat{P}_{ik}^{(1)}(z)$ can be decomposed into the difference between the DGLAP kernel $\hat{P}_{ik}^{(1),\,\mathrm{AP}}(z)$ and $\delta\hat{P}_{ik}^{(1)}(z)$ given

JHEP07(2024)239

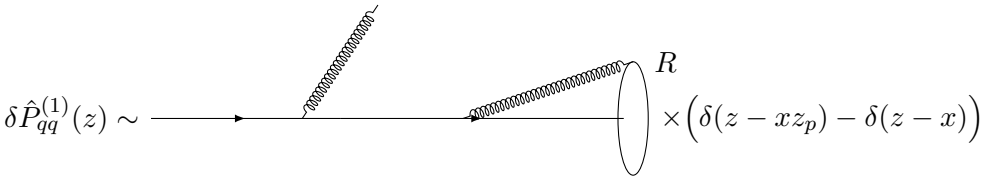

Figure 3. Clustering configuration giving rise to $\delta\hat{P}_{qq}^{(1)}$.

in eq. (2.27). The latter correction originates from the change in the longitudinal momentum fraction of the final state jet in a configuration in which one of the radiated partons clusters with the jet. This scenario is depicted in figure 3 for the $\delta\hat{P}_{qq}^{(1)}$ case. In this configuration, the emission outside the jet will have a coupling evaluated at a scale μ^2 that runs between E^2R^2 and E^2. Conversely, the scale of the coupling associated with the emission inside the jet is bounded by E^2R^2 due to the constraint imposed by the jet radius on the angle of the emission. Therefore, the two terms defining $\hat{P}_{ik}^{(1)}(z)$ in eq. (2.25) enter the NLL evolution equation evaluated at two different scales, that is as

$$\alpha_s(\mu^2)\left(\alpha_s(\mu^2)\hat{P}_{ik}^{(1),\,\mathrm{AP}} - \alpha_s(E^2R^2)\delta\hat{P}_{ik}^{(1)}\right) . \tag{2.29}$$

The above result is explicitly derived in appendix C using the formalism of ref. [22] and it justifies the anomalous dimension given in eq. (2.3), where the term in the second line has the role of changing the scale of the $\delta\hat{P}_{ik}^{(1)}$ term to E^2R^2.

3 Fixed order test through $\mathcal{O}(\alpha_s^2)$

To test our prediction for the inclusive micro-jet spectrum, we compare the perturbative expansion of eq. (2.1) to a fixed-order prediction obtained with the program Event2 [36]. We define the quantity

$$\Delta_i(z,R) \equiv \frac{1}{\sigma_0}\left(\left.\frac{d\sigma^{\mathrm{jet}}}{dz}\right|^{(i)}_{\textsc{Event2}} - \left.\frac{d\sigma^{\mathrm{jet}}}{dz}\right|^{(i)}_{\text{Eq. (2.1)}}\right) , \tag{3.1}$$

where the super-script (i) indicates the perturbative order $\mathcal{O}(\alpha_s^i)$ of the expansion.

We start by considering the $\mathcal{O}(\alpha_s)$ expansion, and in figure 4 (left plot) we plot $\Delta_1(z,R_1)$ for $R_1 = 0.01$. The small value of R_1 allows us to neglect subleading power corrections in R_1 in the theoretical prediction. As expected, the result is consistent with zero within the statistical fluctuations of Event2, in line with an NLL prediction for the inclusive micro-jet spectrum. We then move to $\mathcal{O}(\alpha_s^2)$. At this order, an NLL prediction is expected to capture correctly all logarithmic terms $\ln R^2$, but not the R-independent constant terms. In this case, it is convenient to define a second quantity as

$$\Delta_2(z,R_1,R_2) \equiv \Delta_2(z,R_1) - \Delta_2(z,R_2) . \tag{3.2}$$

Because of the difference between two jet radii, the quantity $\Delta_2(z,R_1,R_2)$ does not contain the $\mathcal{O}(\alpha_s^2)$ constant terms at leading power in the limit $R^2 \ll 1$, which are beyond our accuracy (i.e. NNLL) in this study. In the following, we show $\Delta_2(z,R_1,R_2)$ for $R_1 = 0.01$ and

JHEP07(2024)239

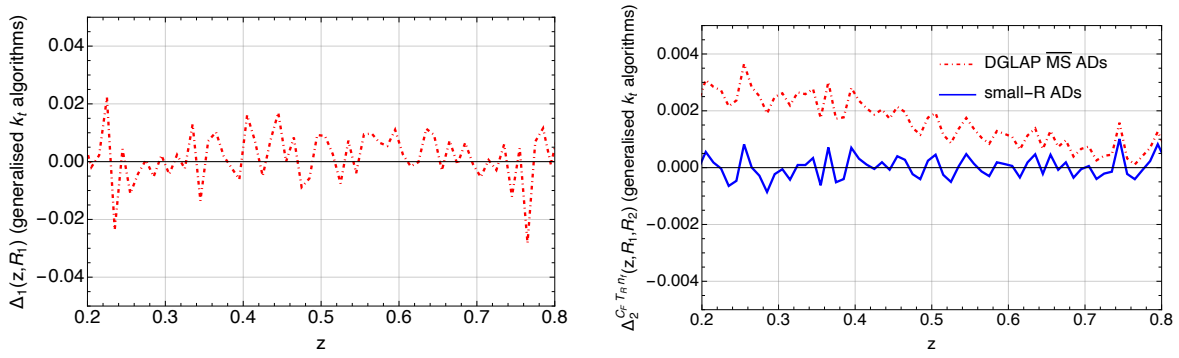

Figure 4. Left: function $\Delta_1(z, R_1)$ displaying the difference with the fixed-order prediction at $\mathcal{O}(\alpha_s)$. Right: function $\Delta_2(z, R_1, R_2)$ displaying the difference with the fixed-order prediction at $\mathcal{O}(\alpha_s^2)$ for the $C_F\, T_R\, n_f$ colour channel.

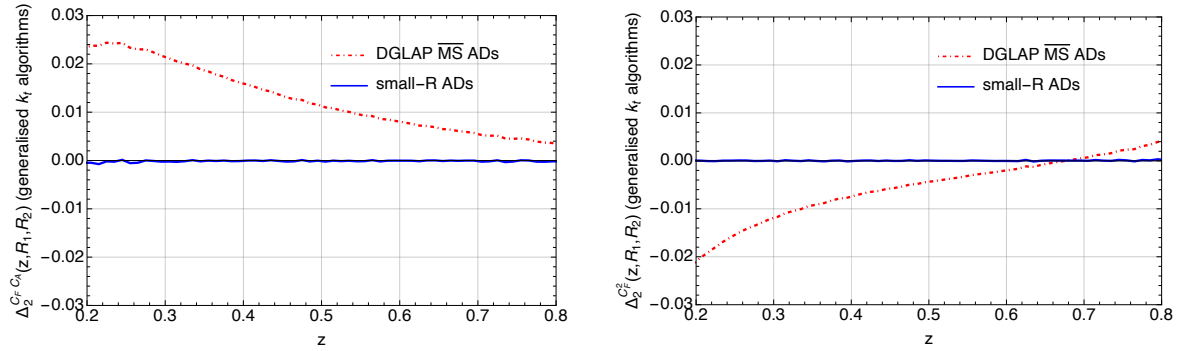

Figure 5. Left: function $\Delta_2(z, R_1, R_2)$ displaying the difference with the fixed-order prediction at $\mathcal{O}(\alpha_s^2)$ for the $C_F\, C_A$ colour channel. Right: function $\Delta_2(z, R_1, R_2)$ displaying the difference with the fixed-order prediction at $\mathcal{O}(\alpha_s^2)$ for the C_F^2 colour channel.

$R_2 = 0.005$, separately for each of the colour structures, that is C_F^2, $C_F\, T_R\, n_f$, $C_F\, C_A$. These are displayed in figure 4 (right plot) and figure 5. In these figures, the red, dot-dashed line represents the prediction obtained by using the standard NLO DGLAP anomalous dimensions in the $\overline{\text{MS}}$ scheme in eq. (2.2). On the other hand, the blue, solid line represents our prediction, obtained by using the $\hat{P}_{ik}$ kernels in the anomalous dimension matrix. From the plots, we clearly observe that the DGLAP-like prediction for $\Delta_2(z, R_1, R_2)$ is incompatible with zero. Instead, the new anomalous dimensions obtained in this article lead to an excellent agreement with the fixed order expectation within the statistical fluctuations of EVENT2 over a very wide range of z. At the edges of the z range we noticed a deviation between our prediction from eq. (2.1) and EVENT2. This is related to subleading-power terms in R present in the latter fixed-order prediction, which exhibit a divergent behaviour near the endpoints $z = 0$ and $z = 1$. These are particularly pronounced in the C_F^2 and $C_F\, C_A$ channels, where the splitting kernels are divergent either at one of or both of the endpoints. Eliminating this feature would require evaluating $\Delta_2(z, R_1, R_2)$ at very small values of R_1 and R_2, which due to numerical stability (as well as to the presence of technical cutoffs) in EVENT2 is very challenging. For this reason we cut the region near the extremities of the z range in the plots.

JHEP07(2024)239

3.1 Anomalous dimensions for alternative jet algorithms: small-$y_{\rm cut}$ jets

It is instructive to investigate the dependence of the FF's anomalous dimension on the kinematic cut applied on jets. Specifically, in addition to the case of inclusive Cambridge-Aachen jets considered so far, we also study Cambridge jets [40] with a small $y_{\rm cut}$. The FF in the latter case is defined by ordering proto-jets according to their angular distance and then cluster them according to the k_t measure. This means that two proto-jets i and j are recombined into a single jet if

$$y_{ij} = 2\,\frac{\min\{E_i^2, E_j^2\}}{Q^2}\,(1-\cos\theta_{ij}) < y_{\rm cut}\,, \tag{3.3}$$

or else the less energetic of the two defines a jet and it is removed from the proto-jets list. This procedure amounts to setting a transverse momentum cut on the final state jets, as opposed to an angular cut as in the small-R case. We repeated the calculation of section 2 for this variant of the FF and found that in this case the NLL result differs from the small-R one both at the level of the boundary conditions to the evolution equation (2.2) as well as at the level of the anomalous dimensions. Remarkably, we find that the anomalous dimensions now coincide with the standard DGLAP ones in the $\overline{\rm MS}$ scheme, while the boundary conditions are given by:

$$\begin{aligned}
D_q^{\rm jet\,(0)}&(z, E\sqrt{y_{\rm cut}}, E\sqrt{y_{\rm cut}}) = \\
&= \frac{C_F}{2}\left(3 - 4\,z + z^2 + 4\,(1+z^2)\,\ln\frac{\min\{1-z,z\}}{1-z}\right)\left(\frac{1}{1-z}\right)_+ \\
&\quad - \frac{C_F}{2\,z\,(1-z)}\Big(4\,(2-3\,z+3\,z^2)\,\ln\,z \\
&\quad + (1-z)\left((5-z)\,z - 4\,(2-2\,z+z^2)\,\ln\frac{\min\{1-z,z\}}{1-z}\right)\Big) \\
&\quad - \frac{C_F}{6}\left(2\,\pi^2 - 3\,(7 - 6\,\ln 2)\right)\,\delta(1-z) - 2\,(\hat{P}_{qq}(z) + \hat{P}_{gq}(z))\,\ln 2\,,
\end{aligned} \tag{3.4}$$

$$D_{\bar q}^{\rm jet\,(0)}(z, E\sqrt{y_{\rm cut}}, E\sqrt{y_{\rm cut}}) = D_q^{\rm jet\,(0)}(z, E\sqrt{y_{\rm cut}}, E\sqrt{y_{\rm cut}})\,, \tag{3.5}$$

$$\begin{aligned}
D_g^{\rm jet\,(0)}&(z, E\sqrt{y_{\rm cut}}, E\sqrt{y_{\rm cut}}) = -4\,T_R\,n_f\,z\,(1-z) \\
&\quad - 4\,\frac{C_A(1-z+z^2)^2 + T_R\,n_f\,z\,(1-3\,z+4\,z^2-2\,z^3)}{(1-z)\,z}\,\ln\frac{(1-z)\,z}{\min\{1-z,z\}} \\
&\quad + \frac{1}{36}\left(C_A\left(131 - 12\,\pi^2 - 132\,\ln 2\right) - 2\,T_R\,n_f\,(17 - 24\,\ln 2)\right)\,\delta(1-z) \\
&\quad - \left(2\,\hat{P}_{gg}(z) + 4\,n_f\,\hat{P}_{qg}(z)\right)\ln 2\,.
\end{aligned} \tag{3.6}$$

In figure 6 we show the small-$y_{\rm cut}$ counterpart to the difference (3.2) between the fixed-order calculation at $\mathcal{O}(\alpha_s^2)$ obtained with Event2 and our analytic prediction. We use $y_{\rm cut,1} = 0.005^2$ and $y_{\rm cut,2} = 0.001^2$ in our test, and find perfect agreement between the two predictions. These findings suggest that the DGLAP anomalous dimension in the $\overline{\rm MS}$ scheme is in one-to-one correspondence with a transverse momentum cut on final-state jets. This observation is important in the context of reproducing DGLAP evolution beyond LL in parton showers, which inevitably use a kinematic cutoff on the generated radiation.

JHEP07(2024)239

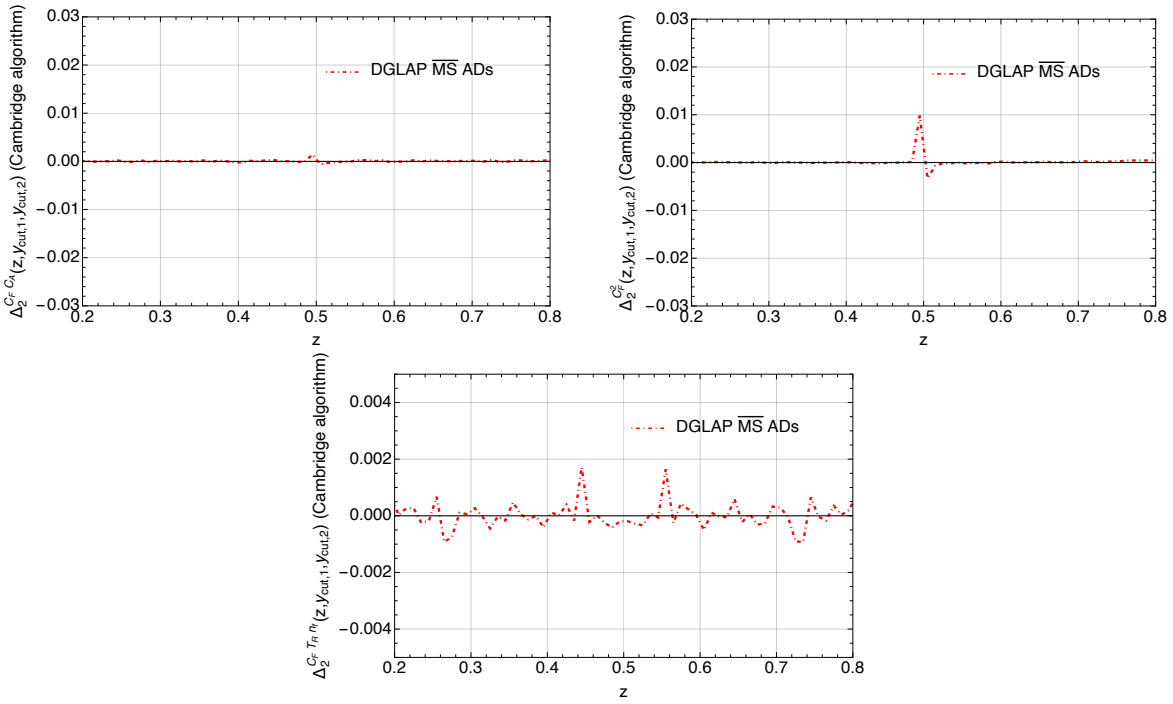

Figure 6. Function $\Delta_2(z, y_{\text{cut},1}, y_{\text{cut},2})$ for different colour factors.

3.1.1 A simple recipe to encode the small-R evolution kernels into the DGLAP equation

We can exploit the calculation performed in the previous section to explore an idea similar in spirit to the one suggested in ref. [33] to absorb the new terms in the two-loop evolution kernels of the small-R FF into a redefinition of the evolution cutoff. In particular, we consider modifying the collinear cutoff in the small-R resummation with a transverse-momentum scale $\mu = z\,ER$, with z being the longitudinal momentum fraction carried by the jet. Specifically, the latter scale represents the maximum transverse momentum carried by emissions within the jet. We then evaluate the evolution equation (2.2) starting from a low scale $\mu = z\,ER$ up to a high scale $\mu = E$. As a consequence of this change of initial scale, the small-R coefficient functions (2.6) are modified accordingly and the $\ln z$ terms in these equations get absorbed into the running of the coupling. In this case, we verified that the anomalous dimensions match the DGLAP/small-y_{cut} ones, hence leading to a evolution equation for these fragmentation functions at the NLL order that coincides with the DGLAP equation. It is important to stress that, in this prescription for the collinear cut-off, the fraction z is that of the final jet, and not that of an intermediate state in the branching history implying that this fraction does not enter the convolutions. We have explicitly verified that the prescription of using standard DGLAP evolution with the zR dependent cut-off, agrees with our small-R evolution equation at NLL order.[5] The above finding is a further confirmation

[5]A crucial identity needed for the verification is the following simple result for a chain of convolutions of identical splitting functions: $(\hat{P}_{ik}^{(0)}(z_1) \otimes \hat{P}_{ik}^{(0)}(z_2) \otimes \ldots \otimes (\ln z_n \hat{P}_{ik}^{(0)}(z_n)))(z) = \frac{1}{n} \ln z\,(\hat{P}_{ik}^{(0)}(z_1) \otimes \hat{P}_{ik}^{(0)}(z_2) \otimes \ldots \otimes \hat{P}_{ik}^{(0)}(z_n))(z)$.

JHEP07(2024)239

of the observation made in the previous section, of an intimate correspondence between the $\overline{\text{MS}}$ scheme and a transverse momentum cutoff. While the zR cut-off prescription restores a standard DGLAP form for the evolution equation, it involves resumming logarithms of zR rather than purely those in R. Hence while it works at NLL to capture the logarithms of R, it also introduces potentially uncontrolled logarithms of z into the final result.

The prescription of starting the evolution at a scale proportional to $z\,R$ concurs with the result of the formalism of ref. [13], provided one also resums the logarithms of z consistently in the evolution equations. Specifically, in addition to evolving the jet function between the scales $z\,R\,E$ and $z\,E$, as done in ref. [13], it is crucial to evolve the hard function between E and $z\,E$ in order to get a full NLL resummation of small-R logarithms. We note that this peculiar additional resummation of logarithms of z necessary to bring the evolution equation into a DGLAP form would not be necessary in the case of small-y_{cut} jets treated in the previous section.

Furthermore, our result provides a crucial insight in the context of reproducing DGLAP within a parton shower beyond LL. In this case, the shower algorithm would operate with a cutoff related to the kinematics of the intermediate state and to the evolution variable. The simple recipe discussed in this section of stopping the evolution at a scale proportional to $z\,R$ would then not be viable, in that one does not have access to the final jet's z fraction during the showering process. We will present an in-depth discussion of this point within a concrete shower algorithm in a forthcoming publication.

4 Conclusions

With the eventual goal of testing a recent formulation of collinear evolution using a generating functional method [22] in mind, in this paper we have analysed the fragmentation function of small-R jets at NLL order, via a fixed-order calculation at two loop order. Here we performed for the first time a two loop calculation of the FF in the presence of the angular cutoff set by the jet radius, and found a difference in the two-loop anomalous dimension for small-R FFs relative to the standard DGLAP ones in the $\overline{\text{MS}}$ scheme.

We have shown a calculation for the inclusive microjet spectrum at NLO in the limit $R \ll 1$, focusing on the C_F^2 colour channel, which is sufficient to infer the general form of the deviation from the standard DGLAP anomalous dimensions in all colour channels. This in turn allowed us to determine the anomalous dimensions for small-R jets at the two loop order. We confirmed our conclusions by comparing to a numerical calculation from the fixed-order program Event2 at $\mathcal{O}(\alpha_s^2)$. An important first remark is that these findings are not just specific to the Cambridge-Aachen algorithm but apply to all members of the generalised k_t family of algorithms, widely used at hadron colliders. For the SISCone algorithm, the only difference at this logarithmic order is encoded in the one-loop boundary condition of the evolution equation (2.2) for the small-R FF. Finally, the result reported here agrees with the second-order expansion of the generating functional given in ref. [22], thereby validating this method for the fragmentation of small-R jets. The derivation is outlined in appendix C.

Moving forward, it is interesting to observe that the simple form of the difference between the small-R and timelike DGLAP anomalous dimensions amounts to terms of the same form as that responsible for the violation of the Gribov-Lipatov reciprocity relation, which has

JHEP07(2024)239

also been previously linked to a change of the kinematic cutoff [33]. To investigate what this implies in the case of the FF we also performed a two loop calculation for an alternative FF measured on Cambridge jets with a transverse momentum cut ($y_{\rm cut}$), as well as for the small-R FF with a cutoff that represents the maximum possible transverse momentum of emissions in the jet, proportional to $z\,R$. Remarkably, in these cases we find that, besides a difference in the one-loop boundary conditions, the two loop anomalous dimensions now coincide with the DGLAP ones in the $\overline{\rm MS}$ scheme. This highlights a correspondence between $\overline{\rm MS}$ and a transverse momentum cut, which is critical to reproduce DGLAP evolution at higher orders with parton showers. Ultimately, it will also be important to assess the effect of our finding in the context of the phenomenology of small-R jets at the LHC and future colliders, in view of the high precision that will be reached in the study of the structure of hadronic jets.

Acknowledgments

We thank Gavin Salam for valuable discussions during the course of this project. This work has been partly funded by the European Research Council (ERC) under the European Union's Horizon 2020 research and innovation program (grant agreement No 788223) (MvB, MD, BKE, JH) and by the U.K.'s Science and Technologies Facilities Council under grant ST/T001038 and ST/X00077X/1 (MD). The work of PM is funded by the European Union (ERC, grant agreement No. 101044599, JANUS). Views and opinions expressed are however those of the authors only and do not necessarily reflect those of the European Union or the European Research Council Executive Agency. Neither the European Union nor the granting authority can be held responsible for them. MD and PM would like to thank the Erwin-Schrödinger-Institute for Mathematics and Physics, for their hospitality while part of this work was being carried out. We also thank each other's institutions for their hospitality at different stages of this project. Finally, we would like to dedicate this article to the memory of Stefano Catani. Like for many topics in QCD, his seminal work underpins our results here, in particular through our direct use of the triple-collinear splitting functions to derive our main results.

A Phase space parametrisation

In this appendix we provide the parametrisation of the three body phase space used throughout the calculations in the article. In $D = 4 - 2\epsilon$ dimensions, the phase space $d\Phi_3$ reads

$$d\Phi_3 = \frac{1}{\pi}\frac{E^{4-4\epsilon}}{(4\pi)^{4-2\epsilon}\Gamma(1-2\epsilon)} dz_2 dz_3 d\theta_{13}^2 d\theta_{23}^2 d\theta_{12}^2 (z_1 z_2 z_3)^{1-2\epsilon} \Delta^{-1/2-\epsilon}\,\Theta(\Delta)\ , \tag{A.1}$$

where the Gram determinant is given by

$$\Delta = 4\theta_{ik}^2\theta_{jk}^2 - \left(\theta_{ij}^2 - \theta_{ik}^2 - \theta_{jk}^2\right)^2, \quad i \neq j \neq k\,, \tag{A.2}$$

and

$$\sum_{i=1}^{3} z_i = 1\,. \tag{A.3}$$

JHEP07(2024)239

We can now introduce the parametrisation of figure 2, for which the phase space measure becomes

$$d\Phi_3^{(B)} \equiv \frac{x}{\pi}\frac{E^{4-4\epsilon}}{(4\pi)^{4-2\epsilon}\Gamma(1-2\epsilon)} dx dz_p d\theta_{13}^2 d\theta_{23}^2 d\theta_{12}^2 ((1-x)x^2(1-z_p)z_p)^{1-2\epsilon}\Delta^{-1/2-\epsilon}\,\Theta(\Delta)\,. \tag{A.4}$$

Similarly, for the parametrisation of figure 1 we obtain

$$d\Phi_3^{(A)} \equiv \frac{1-x}{\pi}\frac{E^{4-4\epsilon}}{(4\pi)^{4-2\epsilon}\Gamma(1-2\epsilon)} dx dz_p d\theta_{13}^2 d\theta_{23}^2 d\theta_{12}^2 ((1-x)^2x(1-z_p)z_p)^{1-2\epsilon}\Delta^{-1/2-\epsilon}\,\Theta(\Delta)\,. \tag{A.5}$$

B Two loop anomalous dimensions for small-R fragmentation

In this appendix we report the explicit anomalous dimensions governing the fragmentation of small-R jets. Starting from the equation (2.25), for quark fragmentation we obtain:

$$\begin{aligned}
\delta\hat{P}_{qq}^{(1)}(z) &= C_F^2\,\ln z\,\frac{1+z\,(4+z)+4\,(1+z^2)\,\ln(1-z)-(1+3z^2)\,\ln z}{1-z} \\
&\quad + 2\,C_F\,T_R\,n_f\,\frac{13\,(1-z^3)+3\ln z\,(4+3\,z\,(2+z)+3\,z\,(1+z)\,\ln z)}{9z}\,, \qquad \text{(B.1)}\\
\delta\hat{P}_{\bar{q}q}^{(1)}(z) &= 2\,C_F\,T_R\,n_f\,\frac{13\,(1-z^3)+3\ln z\,(4+3\,z\,(2+z)+3\,z\,(1+z)\,\ln z)}{9z}\,, \qquad \text{(B.2)}\\
\delta\hat{P}_{gq}^{(1)}(z) &= C_F^2\frac{1}{3z}\Big(3\,(5-z)\,(1-z)-2\,\pi^2\,(2-(2-z)\,z)+12\,(2-(2-z)\,z)\,\mathrm{Li}_2(z) \qquad \text{(B.3)}\\
&\quad + 3\ln z\,(4\,(2-(2-z)\,z)\,\ln(1-z)+z\,(6-2\,z+(2-z)\,\ln z))\Big) \\
&\quad - 4\,C_F\,T_R\,n_f\frac{(2-(2-z)\,z)\,\ln z}{3z} \\
&\quad + C_F\,C_A\,\frac{1}{9z}\Big(6\,\pi^2\,(2-(2-z)\,z)-(1-z)\,(71+z\,(17+26\,z)) \\
&\quad + 3\,\ln z\,\Big(-22-5\,z\,(2-z)-12\,(1+z+z^2)\,\ln z\Big)-36\,(2-(2-z)\,z)\,\mathrm{Li}_2(z)\Big)\,.
\end{aligned}$$

JHEP07(2024)239

Similarly, for gluon fragmentation we obtain:

$$\delta\hat{P}^{(1)}_{gg}(z) = -C_A^2\,\frac{2\,\ln z}{3\,(1-z)\,z}\Big(11 - 18\,z + 3\,z^2 - 18\,z^3 + 11\,z^4 - 12\,(1-z+z^2)^2\,\ln(1-z) + 6\,(1+3\,z^2-4\,z^3+z^4)\,\ln z\Big) - 8\,C_A\,T_R\,n_f\,\frac{(1-z+z^2)^2\,\ln z}{3\,(1-z)\,z} + C_F\,T_R\,n_f\,\left(-\frac{52}{9}\frac{1-z^3}{z} - \frac{4}{3}\left(3+6\,z+4\,z^2\right)\,\ln z + 4\,(1+z)\,\ln^2 z\right), \tag{B.4}$$

$$\delta\hat{P}^{(1)}_{qg}(z) = \delta\hat{P}^{(1)}_{\bar{q}g}(z) = C_F\,T_R\,n_f\,\Big(1 - 6\,z + 5\,z^2 + \frac{2}{3}\,\pi^2\,(1-2\,z+2\,z^2) + (1-2\,z)\,\ln z - (1-2\,z+4\,z^2)\,\ln^2 z - (4-8\,z+8\,z^2)\,\mathrm{Li}_2(z)\Big) + C_A\,T_R\,n_f\,\frac{1}{9}\Big(-9 - 6\,\pi^2 + \frac{26}{z} + 54\,z + 12\,\pi^2\,z - 71\,z^2 - 12\,\pi^2\,z^2 + \frac{6\,\ln z}{z}\left(4 + 6\,z + 18\,z^2 - 9\,z^3 + 6\,z\,(1-2\,z+2\,z^2)\,\ln(1-z)\right) + 18\,(1+4\,z)\,\ln^2 z + 36\,\left(1-2\,z+2\,z^2\right)\,\mathrm{Li}_2(z)\Big). \tag{B.5}$$

C Derivation of two loop anomalous dimensions from $B_2^q(z)$

In this appendix we discuss the derivation of the two loop FF for small-R jets from the generating functionals formalism [10, 24–26, 48] extended to NLL in ref. [22]. This derivation summarises the original calculation of the small-R anomalous dimension, which led us to uncover the discrepancy with the timelike DGLAP case. It also serves as an important test of the method of ref. [22].

We work in the non-singlet (NS) case to simplify the notation, but analogous considerations hold for the other flavour channels. Our starting point is the definition of the NS FF in terms of the quark generating functional $G_q(x,t)$, where t is the evolution time (cf. eq. (2.1) of ref. [22]). This is related to a resolution scale (angle) $\mu = E\,\theta$ by

$$t = \int_{\mu^2}^{E^2} \frac{d\mu'^2}{\mu'^2}\,\frac{\alpha_s(\mu'^2)}{2\pi}\,, \tag{C.1}$$

where $E = Q/2$ is the energy of the initial fragmenting parton (quark in the NS case). The FF can be obtained by taking the derivatives of the quark generating functional G_q w.r.t. the probing function [24–26] (source) u which has the function of tagging a final state parton.

We start with LL for the sake of simplicity, and then discuss the NLL case. The evolution of G_q with the evolution time t is driven by the integral equation

$$G_q(x,t) = u\,\Delta_q(t) + \int_t^{t_0} dt' \int_{z_0}^{1-z_0} dz\,P_{qq}(z)\,G_q(x\,z,t')\,G_g(x\,(1-z),t')\,\frac{\Delta_q(t)}{\Delta_q(t')}\,, \tag{C.2}$$

JHEP07(2024)239

where $P_{qq}(z) = C_F(1+z^2)/(1-z)$ denotes the unregularised $q \to qg$ LO splitting function and $\Delta_q(t)$ is the Sudakov form factor defined as[6]

$$\ln \Delta_q(t) = -\int_t^{t_0} dt' \int_{z_0}^{1-z_0} dz\, P_{qq}(z)\,. \tag{C.3}$$

We now proceed to calculate the NS FF. A first simplification comes from observing that the gluons produced in the branching of the quark do not fragment further if one considers the NS channel. For this reason we can approximate G_g with its first order expansion

$$G_g = u + \mathcal{O}(\alpha_s)\,, \tag{C.4}$$

hence neglecting any radiative corrections. This implies that the evolution of G_q in the NS channel simply amounts to a sequence of angular-ordered primary gluon emissions off the fragmenting quark. The small-R NS FF at LL is then given by

$$D_{\rm NS}^{\rm jet}(z,\mu,ER) = \sum_n \int dP_n \delta\left(z - \prod_{i=1}^{n-1} z_i\right) \prod_{i=1}^{n-1} \Theta(\theta_i^2 - R^2) = \sum_n D_{\rm NS}^{\rm jet,(n)}(z,\mu,ER)\,. \tag{C.5}$$

The *emission probabilities* dP_n are calculated with the formula

$$\int dP_n \equiv \frac{1}{n!}\frac{\delta^n}{\delta u^n} G_q\Big|_{u=0}\,. \tag{C.6}$$

We define the functional derivative by the above equation to effectively act as an ordinary derivative, whereas kinematic phase-space constraints (e.g. the observable's measurement function) are explicitly added for each dP_n (see eq. (C.5) for the FF case).[7] The delta function in eq. (C.5) fixes the longitudinal momentum of the final state quark to be z. This is easily obtained by noticing that each gluon carries a relative fraction $1 - z_i$ of the momentum of the parent, which sets the energy of the final state quark to E times the product of all z_i fractions. Finally, the theta function in eq. (C.5), with θ_i being the angle of gluon i w.r.t. the final state quark,[8] implements the Cambridge clustering condition. This ensures that we consider only gluons which are not recombined with the quark jet, and hence change the jet's momentum fraction. In terms of the evolution time t, this constraint simply translates to

$$t_i < t_R \equiv \int_{E^2R^2}^{E^2} \frac{d\mu'^2}{\mu'^2}\frac{\alpha_s(\mu'^2)}{2\pi}\,. \tag{C.7}$$

This effectively replaces the collinear cutoff t_0 in eq. (C.2), including in the Sudakov form factor. Similarly, we also take the limit of the IR cutoff $z_0 \to 0$ given the IR safety of the

[6] Cf. eq. (2.5) of ref. [22]. The limits of the collinear ($t_0 \to \infty$) and IR ($z_0 \to 0$) cutoffs are meant to be taken at the level of physical observables. The dependence on the cutoffs for IRC safe observables will cancel against that in the real corrections up to power corrections, made negligible by taking a small numerical cutoff. The latter vanish in the calculation reported here since the limits are taken analytically.

[7] An alternative definition, albeit practically equivalent, of the functional derivative is given in ref. [49].

[8] Due to strong angular ordering, this coincides with the angle w.r.t. the emitter.

JHEP07(2024)239

FF that we are computing. From eq. (C.5) we obtain

$$
\begin{aligned}
D_{\rm NS}^{\rm jet,(1)}(z,\mu,ER) &= \Delta_q(t)\,\delta(z-1)\,, \\
D_{\rm NS}^{\rm jet,(2)}(z,\mu,ER) &= \Delta_q(t)\int_t^{t_R} dt_1 \int_0^1 dz_1 P_{qq}(z_1)\,\delta(z-z_1)\,, \\
D_{\rm NS}^{\rm jet,(3)}(z,\mu,ER) &= \Delta_q(t)\int_t^{t_R} dt_1 \int_{t_1}^{t_R} dt_2 \int_0^1 dz_1\,dz_2 P_{qq}(z_1)P_{qq}(z_2)\,\delta(z-z_1z_2)\,, \\
&\ldots = \ldots\,, \\
D_{\rm NS}^{\rm jet,(n)}(z,\mu,ER) &= \Delta_q(t)\int_t^{t_R} dt_1 \ldots \int_{t_{n-2}}^{t_R} dt_{n-1} \int_0^1 \left(\prod_{i=1}^{n-1} dz_i P_{qq}(z_i)\right)\,\delta\left(z-\prod_{i=1}^{n-1} z_i\right)\,.
\end{aligned}
\tag{C.8}
$$

The scale t in the above equations is related by eq. (C.1) to the upper bound on the angle at which the evolution is stopped. In order for all logarithmic terms to be resummed in the FF we set the final scale to $\mu = E$ corresponding to the final $t = 0$. We further introduce the quantity

$$
\Sigma(z,t) \equiv \sum_\ell \int_t^{t_R} dt_1 \ldots \int_{t_{\ell-1}}^{t_R} dt_\ell \int_0^1 \left(\prod_{i=1}^{\ell} dz_i P_{qq}(z_i)\right)\,\delta\left(z-\prod_{i=1}^{\ell} z_i\right)\,,
\tag{C.9}
$$

which allows us to write the NS FF at LL as

$$
D_{\rm NS}^{\rm jet}(z,\mu,ER) = \Delta_q(t)\,(\delta(z-1)+\Sigma(z,t))\,.
\tag{C.10}
$$

What we are interested in here is the evolution of $D_{\rm NS}^{\rm jet}(z,\mu,ER)$ w.r.t. the resolution scale μ. This is related to the evolution in t by

$$
\frac{d}{d\ln\mu^2} = -\frac{\alpha_s(\mu^2)}{2\pi}\,\frac{d}{dt}\,.
\tag{C.11}
$$

We can then obtain the evolution equation for the FF by acting with the above derivative on $D_{\rm NS}^{\rm jet}(z,\mu,ER)$. We arrive at

$$
\begin{aligned}
\frac{dD_{\rm NS}^{\rm jet}(z,\mu,ER)}{d\ln\mu^2} &= \frac{\alpha_s(\mu^2)}{2\pi}\int_0^1 dy\,P_{qq}(y)\Big[\frac{\Delta_q(t)}{y}\,(\delta(z/y-1)+\Sigma(z/y,t)) \\
&\quad -\Delta_q(t)\,(\delta(z-1)+\Sigma(z,t))\Big] = \frac{\alpha_s(\mu^2)}{2\pi}\int_z^1 \frac{dy}{y}\,(P_{qq}(y))_+\,D_{\rm NS}^{\rm jet}\left(\frac{z}{y},\mu,ER\right)\,.
\end{aligned}
\tag{C.12}
$$

The first term in the above equation arises from the derivative of Σ, while the second from the derivative of the Sudakov Δ_q. The LL evolution equation in eq. (C.12) agrees with the DGLAP equation, upon noticing that the plus prescription acting on the whole unregularised splitting function $P_{qq}(y)$ is fully equivalent to the standard regularised splitting function $\hat{P}_{qq}(y)$.

As a next step, we now derive the corresponding equation at NLL. The starting point is the NLL evolution equation which reads [22]

$$
\begin{aligned}
G_q(x,t) &= u\,\Delta_q(t,x) + \int_t^{t_0} dt' \int_{z_0}^{1-z_0} dz\; G_q(x\,z,t')\,G_g(x\,(1-z),t')\,\frac{\Delta_q(t,x)}{\Delta_q(t',x)}\,\mathcal{P}_q(z,t',x) \\
&\quad + \mathbb{K}_q^{\rm finite}[G_q,G_g]\,,
\end{aligned}
\tag{C.13}
$$

JHEP07(2024)239

where

$$\mathcal{P}_q(z,t',x) \equiv \mathcal{P}_q(z,t') - \frac{\alpha_s(\mu'^2)}{2\pi} P_{qq}(z)\, b_0\, \ln x^2\,. \tag{C.14}$$

Here x is the longitudinal momentum fraction of the quark branching at the angular scale t'. The term proportional to $\ln x^2$ in the r.h.s. of eq. (C.14) has the role of ensuring that the effective scale of the strong coupling is the energy of the parton that is branching multiplied by the angular scale of the branching.[9] The quantities $\mathcal{P}_q(z,t)$ and $\mathbb{K}_q^{\text{finite}}$ are defined in eq. (2.10) and appendix C of ref. [22], respectively, and they are derived from the exact $1 \to 3$ splitting functions and corresponding virtual corrections. Accordingly, the LL Sudakov form factor $\Delta_q(t)$ is also upgraded to NLL and defined as

$$\ln \Delta_q(t,x) = -\int_t^{t_0} dt' \int_{z_0}^{1-z_0} dz\, \mathcal{P}_q(z,t',x)\,. \tag{C.15}$$

A few remarks are in order. The quantity $\mathcal{P}_q(z,t)$, referred to as the inclusive emission probability, encodes the next-to-leading order cross section for the radiation of a gluon of momentum $1-z$ differentially both in z and in the angle between the gluon and the emitting quark. This is encoded in the anomalous dimension $\mathcal{B}_2^q(z)$ obtained in ref. [16]. The additional term $\mathbb{K}_q^{\text{finite}}$ encodes the fully-differential structure of the $1 \to 3$ splitting functions, which corrects the inclusive approximation made in $\mathcal{P}_q(z,t)$. This guarantees a full coverage of the $1 \to 3$ splitting phase space and corresponding splitting functions.

An important comment concerns the clustering condition as implemented in eq. (C.5). As discussed in the main text, in the small-R limit one can neglect any clustering of two or more emissions, in that they would result in a power-suppressed term, as well as the recoil of the jet axis. For this reason, the clustering condition in eq. (C.5) (with θ_i denoting the angle w.r.t. the final state quark) remains valid at NLL. From here we essentially follow the same procedure used in the LL case, with more tedious calculations due to the presence of the extra term $\mathbb{K}_q^{\text{finite}}$. An important difference w.r.t. eq. (C.10) is that, at NLL, the FF receives a contribution from $\mathcal{O}(\alpha_s)$ non-logarithmic terms that are obtained by matching the GFs prediction at $\mathcal{O}(\alpha_s)$ to the calculation of the small-R FF at the same order. This leads to the following expression for the NLL FF in the NS channel

$$D_{\text{NS}}^{\text{jet}}(z,\mu,ER) = \left(1 + \frac{\alpha_s(E^2)}{2\pi}\, D_{q,\,\text{NS}}^{\text{jet}\,(0)}\,(z,ER,ER)\right) \otimes \Delta_q(t)\,(\delta(z-1) + \Sigma(z,t))\,, \tag{C.16}$$

where $\Delta_q(t) \equiv \Delta_q(t,1)$ and $D_{q,\,\text{NS}}^{\text{jet}\,(0)}\,(z,ER,ER)$ is the non-singlet part of the quantity defined in eq. (2.6). It reads

$$\begin{aligned} D_{q,\,\text{NS}}^{\text{jet}\,(0)}\,(z,E\,R,E\,R) = {} & -2\,C_F\,(1+z^2)\left(\frac{\ln(1-z)}{1-z}\right)_+ - C_F\left((1-z) + 2\frac{1+z^2}{1-z}\,\ln z\right) \\ & + C_F\left(\frac{13}{2} - \frac{2}{3}\,\pi^2\right)\delta(1-z)\,. \end{aligned} \tag{C.17}$$

[9] In the case of $\mathcal{P}_q$, we have replaced the argument θ with t to ease the notation. The two quantities are related by eq. (C.1). Moreover, we have explicitly expanded out the term proportional to $\ln x^2$ from the definition of the evolution time w.r.t. the notation of ref. [22] (cf. eq. (2.1) there), as this plays a central role in the derivation shown here.

JHEP07(2024)239

The second term to the right of the convolution sign in eq. (C.16) is the result of the functional derivatives of the quark GF, where the quantity $\Sigma(z,t)$ at NLL is now given by

$$\Sigma(z,t) \equiv \sum_\ell \int_t^{t_R} dt_1 \int_0^1 dz_1 \left(\mathcal{P}_q(z_1,t_1,1)+\chi(z_1,t_1)\right) \frac{\Delta_q(t_1,z_1)}{\Delta_q(t_1,1)} \dots \tag{C.18}$$
$$\times \int_{t_{\ell-1}}^{t_R} dt_\ell \int_0^1 dz_\ell \left(\mathcal{P}_q(z_\ell,t_\ell,z_1 z_2 \dots z_{\ell-1})+\chi(z_\ell,t_\ell)\right) \frac{\Delta_q(t_\ell,z_1 z_2 \dots z_\ell)}{\Delta_q(t_\ell,z_1 z_2 \dots z_{\ell-1})} \delta\left(z-\prod_{i=1}^{\ell} z_i\right).$$

The new kernel χ arises from the functional derivatives of $\mathbb{K}_q^{\text{finite}}$ and, using the notation of the main text, it is given by[10]

$$\chi(z,t) \equiv \frac{1}{2!} \int d\Phi_3^{(A)} \frac{(8\pi\,\alpha_s(E^2\,\theta_{12,3}^2))^2}{s_{123}^2} \langle P \rangle_{C_F\,(C_F-C_A/2)} \Big|_{\epsilon=0} \tag{C.19}$$
$$\times\, \delta(t-t_{12,3})\,\delta(z-z_p(1-x))\Theta(\theta_{12,3}^2-R^2)$$
$$+ \int d\Phi_3^{(B)} (8\pi\,\alpha_s(E^2\,\theta_{13}^2))^2 \left(\frac{1}{s_{123}^2}\langle P\rangle_{C_F^2} - \frac{\mathcal{J}(x,z_p)}{E^4}\frac{P_{qq}^{(0)}(x,\epsilon)}{\theta_{13}^2}\frac{P_{qq}^{(0)}(z_p,\epsilon)}{\theta_{23}^2}\right)\Big|_{\epsilon=0}$$
$$\times\, \delta(t-t_{1,3})\left(\delta(z-z_p x)-\delta(z-x)\right)\Theta(\theta_{13}^2-R^2)\Theta(\theta_{13}^2-\theta_{23}^2),$$

with $\mathcal{J}(x,z_p)$ given in eq. (2.18). To evaluate the derivative w.r.t. $\ln\mu^2$, we make use of the following equation

$$\frac{d\,\Sigma(z,t)}{dt} \simeq -\int_z^1 \frac{dy}{y}\left(\mathcal{P}_q(y,t)+\chi(y,t)\right)\left(\delta\left(\frac{z}{y}-1\right)+\Sigma\left(\frac{z}{y},t\right)\right) \tag{C.20}$$
$$+\,2\,b_0 \int_{E^2R^2}^{\mu^2} \frac{d\mu'^2}{\mu'^2}\frac{\alpha_s^2(\mu'^2)}{(2\pi)^2}\int_z^1\frac{dy}{y}\ln y\,P_{qq}(y)\int_{z/y}^1\frac{dy'}{y'}\left(P_{qq}(y')\right)_+\left(\delta\left(\frac{z}{yy'}-1\right)+\Sigma\left(\frac{z}{yy'},t\right)\right).$$

In eq. (C.20) we have exploited the fact that, at NLL, one only needs to retain a single insertion of the $\ln x^2$ term in eq. (C.14), while one can neglect subleading terms stemming from multiple insertions of this contribution to $\mathcal{P}_q(z,t,x)$. Taking the derivative of eq. (C.16) using eq. (C.11) and (C.20) we obtain the following evolution equation

$$\frac{dD_{\text{NS}}^{\text{jet}}(z,\mu,ER)}{d\ln\mu^2} = \frac{\alpha_s(\mu^2)}{2\pi}\int_z^1\frac{dy}{y}\left[\left(\mathcal{P}_q(y,t)\right)_+ + \chi(y,t)\right]D_{\text{NS}}^{\text{jet}}\left(\frac{z}{y},\mu,ER\right) \tag{C.21}$$
$$-\,b_0\int_{E^2R^2}^{\mu^2}\frac{d\mu'^2}{\mu'^2}\frac{\alpha_s^2(\mu'^2)}{(2\pi)^2}\frac{\alpha_s(\mu^2)}{2\pi}\int_z^1\frac{dy}{y}\int_{z/y}^1\frac{dy'}{y'}2\ln y\,P_{qq}(y)\left(P_{qq}(y')\right)_+ D_{\text{NS}}^{\text{jet}}\left(\frac{z}{yy'},\mu,ER\right)$$
$$\equiv \frac{\alpha_s(\mu^2)}{2\pi}\left[\left(\mathcal{P}_q(z,t)\right)_+ + \chi(z,t) - b_0\int_{E^2R^2}^{\mu^2}\frac{d\mu'^2}{\mu'^2}\frac{\alpha_s^2(\mu'^2)}{(2\pi)^2}\delta\hat{P}_{qq}^{(1)}(z)\right]\otimes D_{\text{NS}}^{\text{jet}}(z,\mu,ER),$$

with $\delta\hat{P}_{qq}^{(1)}(z)$ as defined in eq. (2.23). We now comment on the evolution kernel of r.h.s. of eq. (C.21), and its relationship to the small-R anomalous dimension derived in the main text. A first comment concerns the absence of the colour channels $C_F C_A$ and $C_F T_R n_f$ in eq. (C.19). Let us examine the contribution of the corresponding $1\to 3$ splitting functions to the NS channel. We start by reminding the reader that these channels contribute to the

[10] Eq. (C.19) can be evaluated using the relation $\int \frac{d\theta'^2}{\theta'^2}\delta(t-t') = \int \frac{d\theta'^2}{\theta'^2}\frac{2\pi}{\alpha_s}\theta^2\delta(\theta^2-\theta'^2)$.

JHEP07(2024)239

inclusive emission probability $\mathcal{P}_q(z,t)$ via the integral of the corresponding $1 \to 3$ splitting functions with the longitudinal momentum of the quark after the first splitting fixed. For the $C_F C_A$ and $C_F T_R n_f$ channels, this corresponds to fixing the longitudinal momentum fraction of the final quark with the same flavour as the one that initiated the fragmentation. This can be intuitively understood by looking at figure 1 for the $C_F T_R n_f$ channel, where the momentum fraction z_3 is kept fixed (and analogously for the $C_F C_A$ term). On the other hand, the function $\chi(z,t)$ arises from the functional derivatives of $\mathbb{K}_q^{\text{finite}}$, which is sensitive to the differential structure to the $1 \to 3$ splitting. This acts as a correction to the inclusive approximation made in the definition of $\mathcal{P}_q(z,t)$. Since in the NS channel we tag the final state quark, no correction from $\mathbb{K}_q^{\text{finite}}$ survives if the final state quark coincides with the quark after the first splitting, as it is the case for the $C_F C_A$ and $C_F T_R n_f$ contributions. As a consequence, the only contribution from these colour factors is encoded in $\mathcal{P}_q(z,t)$.

A second important comment about eq. (C.21) is the resummation scheme [50] used in the evolution of the generating functionals. As discussed in ref. [22], eq. (C.21) is defined in a resummation scheme in which all non-logarithmic terms, captured in the matching coefficient are evaluated at the hard scale $\mu \sim E$. This is reflected in eq. (C.16), where the non-logarithmic terms $D_{q,\,\text{NS}}^{\text{jet}\,(0)}(z, ER, ER)$ are evaluated at the hard scale. This implies that the logarithmic terms that would be otherwise generated by the running of the low-energy boundary conditions to the evolution equation (2.2) are already encoded in the kernel of eq. (C.21) rather than in the boundary conditions. Specifically, this means that the for the solutions to eq. (C.21) and eq. (2.2) (in the NS channel) to be equivalent, we must verify that

$$\frac{\alpha_s(\mu^2)}{2\pi}\left[\left(\mathcal{P}_q(z,t)\right)_+ + \chi(z,t)\right] = \frac{\alpha_s(\mu^2)}{2\pi}\hat{P}_{qq}^{(0)}(z) + \frac{\alpha_s^2(\mu^2)}{(2\pi)^2}\left(\hat{P}_{qq}^{(1),\,\text{NS}}(z) + b_0\, D_{q,\,\text{NS}}^{\text{jet}\,(0)}(z, ER, ER)\right), \tag{C.22}$$

where $b_0 = 11/6\, C_A - 2/3\, T_R\, n_f$.[11] Since we are working with the NS channel, now $\hat{P}_{qq}^{(1),\,\text{NS}}$ only contains the NS contributions, i.e.

$$\hat{P}_{qq}^{(1),\,\text{NS}}(z) \equiv \hat{P}_{qq}^{(1),\,\text{V}}(z) - \delta\hat{P}_{qq}^{(1)}(z)\,, \tag{C.23}$$

where $\hat{P}_{qq}^{(1),\,\text{V}}(z)$ denotes the standard regularised time-like splitting function in the NS channel (see e.g. in Chapter 6 of ref. [48]). While this correspondence is trivially true at $\mathcal{O}(\alpha_s)$, in order to establish it at $\mathcal{O}(\alpha_s^2)$ we have verified eq. (C.22) numerically for $z \neq 1$, finding perfect agreement. To analyse the case $z = 1$, we can simply check that eq. (C.22) holds at the integral level (i.e. integrating over $z \in [0,1]$). The integral over z of the l.h.s. amounts to the integral of the first term in eq. (C.19) as everything else vanishes upon integration either because of the plus prescription (for what concerns $(\mathcal{P}_q(z,t))_+$) or due to the difference of δ functions (for the second term in eq. (C.19)). This gives

$$\int_0^1 dz \frac{\alpha_s(\mu^2)}{2\pi}\chi(z,t) = \frac{\alpha_s^2(\mu^2)}{(2\pi)^2} C_F\left(C_F - \frac{C_A}{2}\right)\frac{13 - 2\,\pi^2 + 8\,\zeta_3}{4}\,, \tag{C.24}$$

[11] Note that the terms of eq. (C.21) and eq. (2.2) proportional to $\delta\hat{P}_{qq}^{(1)}(z)$ are trivially in agreement at NLL after integrating over μ' (cf. eq. (C.25)).

JHEP07(2024)239

in agreement with the integral of the NS regularised splitting function, as predicted by eq. (C.22). We can now simplify further the structure of eq. (C.21) by writing, at NLL, the integral over μ' as

$$-b_0 \int_{E^2R^2}^{\mu^2} \frac{d\mu'^2}{\mu'^2} \frac{\alpha_s^2(\mu'^2)}{(2\pi)^2} \simeq \frac{\alpha_s(\mu^2)}{2\pi} - \frac{\alpha_s(E^2R^2)}{2\pi} \,. \tag{C.25}$$

It is now straightforward to see that the last term in the r.h.s. of eq. (C.21) has the role of changing the scale of $\delta\hat{P}_{qq}^{(1)}(z)$ in eq. (C.22) from μ^2 to E^2R^2. For consistency with the notation in the main text we also change the scale of the coupling multiplying the boundary condition $D_{q,\,\mathrm{NS}}^{\mathrm{jet}\,(0)}(z, ER, ER)$ from E^2 to E^2R^2, and thus obtain the final form of the evolution equation for the NS channel

$$\frac{dD_{\mathrm{NS}}^{\mathrm{jet}}(z,\mu,ER)}{d\ln\mu^2} = \frac{\alpha_s(\mu^2)}{2\pi}\left(\hat{P}_{qq}^{(0)}(z) + \frac{\alpha_s(\mu^2)}{2\pi}\hat{P}_{qq}^{(1),\,\mathrm{V}}(z) - \frac{\alpha_s(E^2R^2)}{2\pi}\delta\hat{P}_{qq}^{(1)}\right) \otimes D_{\mathrm{NS}}^{\mathrm{jet}}(z,\mu,ER)\,. \tag{C.26}$$

Analogous considerations apply to the other flavour channels.

We conclude with a final remark. In eqs. (C.1), (C.14) we have expanded out, compared to the notation in eq. (2.1) of ref. [22], the dependence on the momentum fraction x from the coupling constant. One could avoid this expansion and instead directly embed this dependence into the structure of the evolution equation. In this case it is convenient to write an evolution equation in the lower bound of the angular evolution range rather than in the upper one, leading to

$$\begin{aligned}\frac{dD_{\mathrm{NS}}^{\mathrm{jet}}(z,E,\mu)}{d\ln\mu^2} = &-\hat{P}_{qq}^{(0)}(z) \otimes \left(\frac{\alpha_s(z^2\mu^2)}{(2\pi)}\, D_{\mathrm{NS}}^{\mathrm{jet}}(z,E,\mu)\right) \\ &- \hat{P}_{qq}^{(1),\,\mathrm{NS}}(z) \otimes \left(\frac{\alpha_s^2(z^2\mu^2)}{(2\pi)^2}\, D_{\mathrm{NS}}^{\mathrm{jet}}(z,E,\mu)\right)\,,\end{aligned} \tag{C.27}$$

where $\hat{P}_{qq}^{(1),\,\mathrm{NS}}(z)$ is defined in eq. (C.23). This equation can be solved, with the same boundary condition given in eq. (C.8) evaluated at $\mu = E\,R$, by integrating between $\mu = E\,R$ and $\mu = E$. We notice that, in this case, the jet radius R does not appear in the running coupling, but it is encoded in the structure of the differential equation. We have compared the NLL solutions to eqs. (C.26), (C.27), finding complete agreement.

References

[1] V.N. Gribov and L.N. Lipatov, *Deep inelastic e p scattering in perturbation theory*, *Sov. J. Nucl. Phys.* **15** (1972) 438 [INSPIRE].

[2] Y.L. Dokshitzer, *Calculation of the structure functions for deep inelastic scattering and e^+e^- annihilation by perturbation theory in quantum chromodynamics*, *Sov. Phys. JETP* **46** (1977) 641 [INSPIRE].

JHEP07(2024)239

[3] G. Altarelli and G. Parisi, *Asymptotic freedom in parton language*, *Nucl. Phys. B* **126** (1977) 298 [INSPIRE].

[4] W. Furmanski and R. Petronzio, *Singlet parton densities beyond leading order*, *Phys. Lett. B* **97** (1980) 437 [INSPIRE].

[5] G. Curci, W. Furmanski and R. Petronzio, *Evolution of parton densities beyond leading order: the nonsinglet case*, *Nucl. Phys. B* **175** (1980) 27 [INSPIRE].

[6] A. Jain, M. Procura and W.J. Waalewijn, *Parton fragmentation within an identified jet at NNLL*, *JHEP* **05** (2011) 035 [arXiv:1101.4953] [INSPIRE].

[7] S. Alioli and J.R. Walsh, *Jet veto clustering logarithms beyond leading order*, *JHEP* **03** (2014) 119 [arXiv:1311.5234] [INSPIRE].

[8] H.-M. Chang, M. Procura, J. Thaler and W.J. Waalewijn, *Calculating track-based observables for the LHC*, *Phys. Rev. Lett.* **111** (2013) 102002 [arXiv:1303.6637] [INSPIRE].

[9] M. Ritzmann and W.J. Waalewijn, *Fragmentation in jets at NNLO*, *Phys. Rev. D* **90** (2014) 054029 [arXiv:1407.3272] [INSPIRE].

[10] M. Dasgupta, F. Dreyer, G.P. Salam and G. Soyez, *Small-radius jets to all orders in QCD*, *JHEP* **04** (2015) 039 [arXiv:1411.5182] [INSPIRE].

[11] A. Banfi et al., *Jet-vetoed Higgs cross section in gluon fusion at N^3LO+NNLL with small-R resummation*, *JHEP* **04** (2016) 049 [arXiv:1511.02886] [INSPIRE].

[12] M. Dasgupta, F.A. Dreyer, G.P. Salam and G. Soyez, *Inclusive jet spectrum for small-radius jets*, *JHEP* **06** (2016) 057 [arXiv:1602.01110] [INSPIRE].

[13] Z.-B. Kang, F. Ringer and I. Vitev, *The semi-inclusive jet function in SCET and small radius resummation for inclusive jet production*, *JHEP* **10** (2016) 125 [arXiv:1606.06732] [INSPIRE].

[14] H. Chen, I. Moult and H.X. Zhu, *Quantum interference in jet substructure from spinning gluons*, *Phys. Rev. Lett.* **126** (2021) 112003 [arXiv:2011.02492] [INSPIRE].

[15] H. Chen, I. Moult and H.X. Zhu, *Spinning gluons from the QCD light-ray OPE*, *JHEP* **08** (2022) 233 [arXiv:2104.00009] [INSPIRE].

[16] M. Dasgupta and B.K. El-Menoufi, *Dissecting the collinear structure of quark splitting at NNLL*, *JHEP* **12** (2021) 158 [arXiv:2109.07496] [INSPIRE].

[17] M. Dasgupta, B.K. El-Menoufi and J. Helliwell, *QCD resummation for groomed jet observables at NNLL+NLO*, *JHEP* **01** (2023) 045 [arXiv:2211.03820] [INSPIRE].

[18] H. Chen, I. Moult, J. Sandor and H.X. Zhu, *Celestial blocks and transverse spin in the three-point energy correlator*, *JHEP* **09** (2022) 199 [arXiv:2202.04085] [INSPIRE].

[19] H. Chen et al., *Collinear parton dynamics beyond DGLAP*, arXiv:2210.10061 [INSPIRE].

[20] X. Liu and H.X. Zhu, *Nucleon energy correlators*, *Phys. Rev. Lett.* **130** (2023) 091901 [arXiv:2209.02080] [INSPIRE].

[21] W. Chen et al., *NNLL resummation for projected three-point energy correlator*, *JHEP* **05** (2024) 043 [arXiv:2307.07510] [INSPIRE].

[22] M. van Beekveld et al., *Collinear fragmentation at NNLL: generating functionals, groomed correlators and angularities*, *JHEP* **05** (2024) 093 [arXiv:2307.15734] [INSPIRE].

[23] H. Cao, X. Liu and H.X. Zhu, *Toward precision measurements of nucleon energy correlators in lepton-nucleon collisions*, *Phys. Rev. D* **107** (2023) 114008 [arXiv:2303.01530] [INSPIRE].

JHEP07(2024)239

[24] K. Konishi, A. Ukawa and G. Veneziano, *Jet calculus: a simple algorithm for resolving QCD jets*, *Nucl. Phys. B* **157** (1979) 45 [INSPIRE].

[25] A. Bassetto, M. Ciafaloni and G. Marchesini, *Jet structure and infrared sensitive quantities in perturbative QCD*, *Phys. Rept.* **100** (1983) 201 [INSPIRE].

[26] Y.L. Dokshitzer, V.A. Khoze, A.H. Mueller and S.I. Troian, *Basics of perturbative QCD*, (1991).

[27] J.M. Campbell and E.W.N. Glover, *Double unresolved approximations to multiparton scattering amplitudes*, *Nucl. Phys. B* **527** (1998) 264 [hep-ph/9710255] [INSPIRE].

[28] S. Catani and M. Grazzini, *Collinear factorization and splitting functions for next-to-next-to-leading order QCD calculations*, *Phys. Lett. B* **446** (1999) 143 [hep-ph/9810389] [INSPIRE].

[29] V.N. Gribov and L.N. Lipatov, *e^+e^- pair annihilation and deep inelastic ep scattering in perturbation theory*, *Sov. J. Nucl. Phys.* **15** (1972) 675 [INSPIRE].

[30] A.H. Mueller, *Multiplicity and hadron distributions in QCD jets. 2. A general procedure for all nonleading terms*, *Nucl. Phys. B* **228** (1983) 351 [INSPIRE].

[31] B. Basso and G.P. Korchemsky, *Anomalous dimensions of high-spin operators beyond the leading order*, *Nucl. Phys. B* **775** (2007) 1 [hep-th/0612247] [INSPIRE].

[32] Y.L. Dokshitzer and G. Marchesini, *N=4 SUSY Yang-Mills: three loops made simple(r)*, *Phys. Lett. B* **646** (2007) 189 [hep-th/0612248] [INSPIRE].

[33] Y.L. Dokshitzer, G. Marchesini and G.P. Salam, *Revisiting parton evolution and the large-x limit*, *Phys. Lett. B* **634** (2006) 504 [hep-ph/0511302] [INSPIRE].

[34] D. Neill and F. Ringer, *Soft fragmentation on the celestial sphere*, *JHEP* **06** (2020) 086 [arXiv:2003.02275] [INSPIRE].

[35] S. Jadach, A. Kusina, M. Skrzypek and M. Slawinska, *Two real parton contributions to non-singlet kernels for exclusive QCD DGLAP evolution*, *JHEP* **08** (2011) 012 [arXiv:1102.5083] [INSPIRE].

[36] S. Catani and M.H. Seymour, *A general algorithm for calculating jet cross-sections in NLO QCD*, *Nucl. Phys. B* **485** (1997) 291 [hep-ph/9605323] [INSPIRE].

[37] M. Cacciari, G.P. Salam and G. Soyez, *FastJet user manual*, *Eur. Phys. J. C* **72** (2012) 1896 [arXiv:1111.6097] [INSPIRE].

[38] S. Catani, Y.L. Dokshitzer, M.H. Seymour and B.R. Webber, *Longitudinally invariant K_t clustering algorithms for hadron hadron collisions*, *Nucl. Phys. B* **406** (1993) 187 [INSPIRE].

[39] M. Cacciari, G.P. Salam and G. Soyez, *The anti-k_t jet clustering algorithm*, *JHEP* **04** (2008) 063 [arXiv:0802.1189] [INSPIRE].

[40] Y.L. Dokshitzer, G.D. Leder, S. Moretti and B.R. Webber, *Better jet clustering algorithms*, *JHEP* **08** (1997) 001 [hep-ph/9707323] [INSPIRE].

[41] M. Wobisch and T. Wengler, *Hadronization corrections to jet cross-sections in deep inelastic scattering*, in the proceedings of the *Workshop on Monte Carlo generators for HERA physics (plenary starting meeting)*, (1998) [hep-ph/9907280] [INSPIRE].

[42] G.P. Salam and G. Soyez, *A practical seedless infrared-safe cone jet algorithm*, *JHEP* **05** (2007) 086 [arXiv:0704.0292] [INSPIRE].

JHEP07(2024)239

[43] A. Mukherjee and W. Vogelsang, *Jet production in (un)polarized pp collisions: dependence on jet algorithm*, *Phys. Rev. D* **86** (2012) 094009 [*Erratum ibid.* **107** (2023) 119901] [arXiv:1209.1785] [INSPIRE].

[44] Z.-B. Kang, F. Ringer and W.J. Waalewijn, *The energy distribution of subjets and the jet shape*, *JHEP* **07** (2017) 064 [arXiv:1705.05375] [INSPIRE].

[45] P. Nason and B.R. Webber, *Scaling violation in e^+e^- fragmentation functions: QCD evolution, hadronization and heavy quark mass effects*, *Nucl. Phys. B* **421** (1994) 473 [*Erratum ibid.* **480** (1996) 755] [INSPIRE].

[46] G.F.R. Sborlini, D. de Florian and G. Rodrigo, *Double collinear splitting amplitudes at next-to-leading order*, *JHEP* **01** (2014) 018 [arXiv:1310.6841] [INSPIRE].

[47] O. Braun-White and N. Glover, *Decomposition of triple collinear splitting functions*, *JHEP* **09** (2022) 059 [arXiv:2204.10755] [INSPIRE].

[48] R.K. Ellis, W.J. Stirling and B.R. Webber, *QCD and collider physics*, Cambridge University Press, Cambridge, U.K. (2011) [DOI:10.1017/CBO9780511628788] [INSPIRE].

[49] A. Banfi, F.A. Dreyer and P.F. Monni, *Higher-order non-global logarithms from jet calculus*, *JHEP* **03** (2022) 135 [arXiv:2111.02413] [INSPIRE].

[50] S. Catani, D. de Florian and M. Grazzini, *Universality of nonleading logarithmic contributions in transverse momentum distributions*, *Nucl. Phys. B* **596** (2001) 299 [hep-ph/0008184] [INSPIRE].

JHEP07(2024)239